Synthesis of thiosemicarbazones and their organoiodine cocrystals: cooperative effects of halogen and hydrogen bonding

Andrew J. Peloquin, Arianna C. Ragusa, Hadi D. Arman, Colin D. McMillen,* and William T. Pennington*

Department of Chemistry, Clemson University, Clemson, SC 29634-0973, USA

Corresponding author contacts:
William T. Pennington & Colin D. McMillen
H.L. Hunter Laboratories
Clemson, SC 29634
Tel. 864-656-2319
Fax: 864-656-6613
e-mail: billp@clemson.edu & cmcmill@clemson.edu

Synthesis of thiosemicarbazones and their organoiodine cocrystals: cooperative effects of halogen and hydrogen bonding

Andrew J. Peloquin, Arianna C. Ragusa, Hadi D. Arman, Colin D. McMillen,* and William T. Pennington*

Department of Chemistry, Clemson University, Clemson, SC 29634-0973, USA

Abstract

Utilizing the facile addition-elimination reaction of thiosemicarbazide with acetone or aldehydes, nine thiosemicarbazones were synthesized. Aldehydes were chosen which contain additional heteroatoms to increase the diversity of possible intermolecular interactions. Further, the thiosemicarbazone synthesis was conducted in situ with one of the common halogen bond donors 1,2-, 1,3-, or 1,4-diiodotetrafluorobenzene, 1,3,5-trifluoro-2,4,6-triiodobenzene, or tetraiodoethylene. These reactions resulted in the characterization of 12 new cocrystals showcasing halogen bonding. The dimerization of two thiosemicarbazone units through a pair of N–H···S hydrogen bonds was a universal feature of the solid-state structures in this series, with the hydrogen bond network often extending these motifs into chains. The organoiodines serve to link chains through either I···S or I···N halogen bonding, or less commonly, S···I chalcogen bonding. This variety of intermolecular interactions leads to the formation of double-stranded chains, ribbons, and sheets.

Keywords:

Halogen bonding, Hydrogen bonding, Chalcogen bonding, Sulfur-iodine interactions, Iodine

1. Introduction

Halogen bonding, defined by IUPAC as "a net attractive interaction between an electrophilic region associated with a halogen atom in a molecular entity and a nucleophilic region in another, or the same, molecular entity [1]" has drawn more attention in recent years [2–10]. Similar to hydrogen bonding, halogen bonding is strong, selective, and directional. Organic iodines are among the most commonly utilized halogen bond donors [11], in large part due to their greater polarizability. When paired with halogen bond acceptor molecules with a diversity of heteroatoms, the cooperative effects of halogen, chalcogen, and hydrogen bonding can be revealed. One such diverse heteroatom system is that of thiosemicarbazones, formally referred to as hydrazinecarbothioureas. The thiosemicarbazone functionality contains a thione sulfur atom capable of acting as either a halogen bond acceptor, chalcogen bond donor, and/or hydrogen bond acceptor. In addition, three chemically distinct nitrogen atoms are available: the terminal, primary NH_2; a secondary NH; as well as an iminium nitrogen atom. Formed from a facile addition-elimination sequence of thiosemicarbazide and a carbonyl group, additional heteroatoms are easily incorporated into the resulting thiosemicarbazone.[12]

Thiosemicarbazones have been investigated for a wide range of biological applications, including antibacterial, antifungal, antiviral, and anticancer properties.[13–17] A notable example of these antitumor properties were displayed by using aromatic-substituted thiosemicarbazones as ligands for Ni(II), Cu(I), and Ag(I) complexes.[18–20] Depending on the identity of the ancillary ligands, the thiosemicarbazone was found to coordinate the metal center through only the sulfur atom, or a combination of the sulfur and iminium nitrogen atoms. This diversity of coordination behavior is an important feature of thiosemicarbazones, as it has been noted that the biological activity of these compounds is typically enhanced upon coordination to cationic metal ions.[21, 22] Beyond their biological applications, these diverse molecules have also been investigated for their application to ion sensing as well as for their catalytic properties.[23, 24]

Our group has recently been interested in the role of the sulfur atom in I···S halogen and chalcogen bonding interactions as a crystal design tool, as well as their role in the formation of deep eutectic solvents derived from halogen bonding.[25–27] Herein, we report the solid-state structure of nine thiosemicarbazones derived from various ketones and aldehydes (Scheme 1). Of these, seven were isolated as cocrystalline structures with organoiodines. The crystal packing observed in this series is dominated by noncovalent interaction patterns consisting of N–H···S hydrogen bonding, as well as both I···S halogen and chalcogen bonding.

2. Experimental

2.1 Cocrystal synthesis

(2-(1-methylethylidene)hydrazinecarbothiourea)(1,2-diiodo-3,4,5,6-tetrafluorobenzene) (1A): In a 20 mL glass vial, thiosemicarbazide (65 mg, 0.71 mmol) and 1,2-diiodo-3,4,5,6-tetrafluorobenzene (287 mg, 0.71 mmol) were dissolved in hot acetone (10 mL). The solvent was allowed to slowly evaporate under ambient conditions until colorless, block-like crystals were observed.

(2-(1-methylethylidene)hydrazinecarbothiourea)(1,3-diiodo-2,4,5,6-tetrafluorobenzene) (1B): Using the same procedure as **1A**, thiosemicarbazide (61 mg, 0.67 mmol) and 1,3-diiodo-2,4,5,6-tetrafluorobenzene (269 mg, 0.67 mmol) were dissolved in hot acetone (10 mL), yielding colorless, plate-like crystals.

(2-(1-methylethylidene)hydrazinecarbothiourea)(1,4-diiodo-2,3,5,6-tetrafluorobenzene) (1C): Using the same procedure as **1A**, thiosemicarbazide (52 mg, 0.57 mmol) and 1,4-diiodo-2,3,5,6-tetrafluorobenzene (229 mg, 0.57 mmol) were dissolved in hot acetone (10 mL), yielding colorless, plate-like crystals.

(2-(1-methylethylidene)hydrazinecarbothiourea)(1,3,5-trifluoro-2,4,6-triiodobenzene) (1D): Using the same procedure as **1A**, thiosemicarbazide (56 mg, 0.61 mmol) and 1,3,5-trifluoro-2,4,6-trifluorobenzene (313 mg, 0.61 mmol) were dissolved in hot acetone (10 mL), yielding colorless, block-like crystals.

[bis(2-(1-methylethylidene)hydrazinecarbothiourea)](tetraiodoethylene) (1E): Using the same procedure as **1A**, thiosemicarbazide (51 mg, 0.56 mmol) and tetraiodoethylene (149 mg, 0.28 mmol) were dissolved in hot acetone (10 mL), yielding yellow, needle-like crystals of **1E** and colorless, needle-like crystals of **2E**.

[bis(2-(2-thienylmethylene)hydrazinecarbothiourea)][tris(1,4-diiodo-2,3,5,6-tetrafluorobenzene)] (3C): Using the same procedure as **1A**, thiosemicarbazide (71 mg, 0.78 mmol), 2-thiophenecarboxaldehyde (73 μL, 0.78 mmol), and 1,4-diiodo-2,3,5,6-tetrafluorobenzene (470 mg, 1.17 mmol) were dissolved in a mixture of ethanol (8 mL) and water (2 mL), yielding colorless, plank-like crystals.

[bis(2-((4-methyl-5-thiazoyl)methylene)hydrazinecarbothiourea)](1,2-diiodo-3,4,5,6-tetrafluorobenzene) (4A): Using the same procedure as **1A**, thiosemicarbazide (90 mg, 0.99 mmol), 4-methyl-5-thiazolecarboxaldehyde (99 μL, 0.99 mmol), and 1,2-diiodo-3,4,5,6-tetrafluorobenzene (198 mg, 0.49 mmol) were dissolved in a mixture of ethanol (8 mL) and water (2 mL), yielding yellow, plate-like crystals.

[bis(2-((4-methyl-5-thiazoyl)methylene)hydrazinecarbothiourea)](1,4-diiodo-2,3,5,6-tetrafluorobenzene) (4C): Using the same procedure as **1A**, thiosemicarbazide (107 mg, 1.17 mmol), 4-methyl-5-thiazolecarboxaldehyde (1.07

μL, 1.17 mmol), and 1,4-diiodo-2,3,5,6-tetrafluorobenzene (236 mg, 0.59 mmol) were dissolved in a mixture of ethanol (8 mL) and water (2 mL), yielding yellow, block-like crystals.

[bis(2-((4-(3-pyridyl)phenyl)methylene)hydrazinecarbothiourea)](1,4-diiodo-2,3,5,6-tetrafluorobenzene) (5C): Using the same procedure as **1A**, thiosemicarbazide (96 mg, 1.05 mmol), 4-(2-pyridinyl)benzaldehyde (193 mg, 1.05 mmol), and 1,4-diiodo-2,3,5,6-tetrafluorobenzene (212 mg, 0.53 mmol) were dissolved in a mixture of ethanol (8 mL) and water (2 mL), colorless, plate-like crystals.

[bis(2-(3-pyridinylmethylene)hydrazinecarbothiourea)](1,4-diiodo-2,3,5,6-tetrafluorobenzene) (6C): Using the same procedure as **1A**, thiosemicarbazide (104 mg, 1.14 mmol), 3-pyridinecarboxaldehyde (107 μL, 1.14 mmol), and 1,4-diiodo-2,3,5,6-tetrafluorobenzene (229 mg, 0.57 mmol) were dissolved in a mixture of ethanol (8 mL) and water (2 mL), yielding colorless, plate-like crystals.

[bis(2-((2,4,6-trimethoxyphenyl)methylene)hydrazinecarbothiourea)][tris(1,4-diiodo-2,3,5,6-tetrafluorobenzene)] (7C): Using the same procedure as **1A**, thiosemicarbazide (68 mg, 0.75 mmol), 2,4,6-trimethoxybenzaldehyde (146.4 mg, 0.75 mmol), and 1,4-diiodo-2,3,5,6-tetrafluorobenzene (450 mg, 1.12 mmol) were dissolved in a mixture of ethanol (8 mL) and water (2 mL), yielding colorless, prism-like crystals.

2-(benzo[*b*]thien-3-ylmethylene)hydrazinecarbothiourea (8): Using the same procedure as **1A**, thiosemicarbazide (114 mg, 1.25 mmol) and benzo[*b*]thiophene-1-carboxaldehyde (203 mg, 1.25 mmol), were dissolved in a mixture of ethanol (8 mL) and water (2 mL), yielding colorless, prism-like crystals.

2-((4-iodophenyl)methylene)hydrazinecarbothiourea (9): Using the same procedure as **1A**, thiosemicarbazide (63 mg, 0.69 mmol) and 4-iodobenzaldehyde (160 mg, 0.69 mmol), were dissolved in a mixture of ethanol (8 mL) and water (2 mL), yielding colorless, prism-like crystals.

2.2 X-ray structure determination

For single-crystal X-ray analysis, crystals were mounted on low background cryogenic loops using paratone oil. Data were collected using Mo Kα radiation (λ = 0.71073 Å) on either a Bruker D8 Venture diffractometer with an Incoatec Iμs microfocus source and a Photon 2 detector, a Rigaku XtaLAB Synergy diffractometer with a PhotonJet source and a HyPix3000 detector, or a Rigaku AFC8 diffractometer with a sealed tube source and a Mercury CCD detector. Diffraction data were collected using φ and ω-scans and subsequently processed and scaled using the APEX3 (SAINT/SADABS), *CrysAlis PRO* 1.171.40.58, or CrystalClear software suites.[28, 29] The structures were solved with the SHELXT structure solution program and refined utilizing

OLEX2.refine, both incorporated in the *OLEX2* (v1.5) program package.[30–32] The N–H hydrogen atoms were refined with appropriate DFIX restraints, while all other hydrogen atoms were placed in geometrically optimized positions using the appropriate riding models. **2E** was refined as a racemic twin.

Table 1. Crystallographic data and selected data collection parameters for **1A**–**1E** & **2E**

Cocrystal	**1A**	**1B**	**1C**	**1D**	**1E**	**2E**
Empirical formula	$C_{10}H_9F_4I_2N_3S$	$C_{20}H_{18}F_8I_4N_6S_2$	$C_{10}H_9F_4I_2N_3S$	$C_{10}H_9F_3I_3N_3S$	$C_{10}H_{18}I_4N_6S_2$	$C_{15}H_{24}I_5N_3S$
Formula weight (g/mol)	533.06	1066.12	533.06	640.96	794.02	912.93
Crystal system	triclinic	monoclinic	triclinic	orthorhombic	triclinic	orthorhombic
Space group	*P*-1	$P2_1/c$	*P*-1	$Pca2_1$	*P*-1	$P2_12_12_1$
T (K)	106(9)	100.0(3)	100(2)	106(4)	153(2)	100(2)
a (Å)	7.45613(9)	13.3400(2)	7.6616(6)	17.5980(2)	7.2515(15)	9.3001(13)
b (Å)	8.31433(10)	32.8908(3)	13.5819(11)	11.88910(10)	8.3173(17)	16.0123(17)
c (Å)	13.14247(14)	7.17590(10)	15.7300(13)	7.93190(10)	10.103(2)	17.2051(18)
α (°)	107.1070(10)	90	73.818(3)	90	86.40(3)	90
β (°)	103.4195(10)	101.8880(10)	89.878(3)	90	69.40(3)	90
γ (°)	95.4238(9)	90	89.311(3)	90	72.57(3)	90
V (Å^3)	745.727(15)	3080.99(7)	1571.9(2)	1659.55(3)	543.6(2)	2562.1(5)
ρ_{calcd} (g·cm^{-3})	2.374	2.298	2.253	2.565	2.426	2.367
reflns collected	42546	210383	27596	28120	5118	57473
Independent reflns	3295	8179	6166	4133	2117	6067
R(int)	0.0379	0.0818	0.0360	0.0891	0.0414	0.0517
# parameters	195	389	389	194	121	231
R_1 [$I>2\sigma(I)$]	0.0153	0.0503	0.0351	0.0346	0.0588	0.0289
wR_2 [$I>2\sigma(I)$]	0.0351	0.1443	0.0695	0.0700	0.1505	0.0558
R_1 (all)	0.0161	0.0576	0.0456	0.0373	0.0705	0.0374
wR_2 (all)	0.0355	0.1475	0.0777	0.0724	0.1581	0.0614
GooF	1.052	1.212	1.293	1.044	1.089	1.154
Flack parameter	N/A	N/A	N/A	-0.03(2)	N/A	0.49(7)
CCDC #	2117350	2117351	2117352	2117353	2117354	2117355

Table 2. Crystallographic data and selected data collection parameters for **3C**, **4A**, **4C**, **5C**, **6C**, & **7C**

Cocrystal	**3C**	**4A**	**4C**	**5C**	**6C**	**7C**
Empirical formula	$C_{30}H_{14}F_{12}I_6N_6S_4$	$C_{18}H_{16}F_4I_2N_8S_4$	$C_{18}H_{16}F_4I_2N_8S_4$	$C_{32}H_{24}F_4I_2N_8S_2$	$C_{20}H_{16}F_4I_2N_8S_2$	$C_{40}H_{30}F_{12}I_6N_6O_6S_2$
Formula weight (g/mol)	1576.11	802.43	802.43	914.51	762.33	1744.22
Crystal system	triclinic	monoclinic	triclinic	monoclinic	triclinic	monoclinic
Space group	*P*-1	$P2_1/c$	*P*-1	$P2_1/c$	*P*-1	$P2_1/c$
T (K)	106(9)	103(5)	110(3)	99.9(6)	105(7)	100.0(2)
a (Å)	8.91617(10)	19.09476(14)	6.18726(12)	16.6688(4)	7.59115(13)	11.22332(11)
b (Å)	10.28733(11)	7.51016(4)	8.98119(16)	4.44440(10)	8.84386(14)	26.4822(2)
c (Å)	12.31266(12)	19.40945(13)	12.7664(2)	22.2046(5)	10.38104(16)	8.77315(8)
α (°)	75.4357(9)	90	85.4575(14)	90	86.5404(13)	90
β (°)	80.0612(9)	111.2260(8)	81.9103(15)	90.865(2)	69.9891(15)	95.7649(9)
γ (°)	75.4231(10)	90	73.4475(17)	90	74.0906(15)	90
V (Å^3)	1050.66(2)	2594.58(3)	672.68(2)	1644.79(7)	629.341(19)	2594.36(4)
ρ_{calcd} (g·cm^{-3})	2.491	2.054	1.981	1.847	2.011	2.233
reflns collected	64316	170918	33002	31717	24440	91215
Independent reflns	5486	6906	3516	3596	3303	6829
R(int)	0.0947	0.1023	0.0360	0.0536	0.0414	0.0471
# parameters	274	351	389	229	121	340
R_1 [$I>2\sigma(I)$]	0.0276	0.0221	0.0272	0.0285	0.0486	0.0213
wR_2 [$I>2\sigma(I)$]	0.0561	0.0494	0.0540	0.0538	0.1153	0.0431
R_1 (all)	0.0380	0.0256	0.0513	0.0399	0.0763	0.0258
wR_2 (all)	0.0670	0.0508	0.0682	0.0567	0.1493	0.0450
GooF	1.121	1.033	1.134	1.043	1.035	1.045
Flack parameter	N/A	N/A	N/A	N/A	N/A	N/A
CCDC #	2117356	2117357	2117358	2117359	2117360	2117361

Table 3. Crystallographic data and selected data collection parameters for **8** & **9**

Cocrystal	**8**	**9**
Empirical formula	$C_{10}H_9N_3S_2$	$C_8H_8IN_3S$
Formula weight (g/mol)	235.32	305.13
Crystal system	monoclinic	orthorhombic
Space group	$P2_1/c$	*Pbca*
T (K)	105(8)	106(9)
a (Å)	7.6620(2)	8.37047(9)
b (Å)	25.6544(4)	8.39907(9)
c (Å)	5.79570(10)	30.0387(3)
α (°)	90	90
β (°)	105.487(2)	90
γ (°)	90	90
V (Å^3)	1097.86(4)	2111.85(4)
ρ_{calcd} (g·cm^{-3})	1.424	1.919
reflns collected	70858	67914
Independent reflns	2879	2806
R(int)	0.2034	0.0614
# parameters	148	130
R_1 [$I>2\sigma(I)$]	0.0565	0.0202
wR_2 [$I>2\sigma(I)$]	0.1448	0.0469
R_1 (all)	0.0703	0.0226
wR_2 (all)	0.1512	0.0481
GooF	1.043	1.087
Flack parameter	N/A	N/A
CCDC #	2117362	2117363

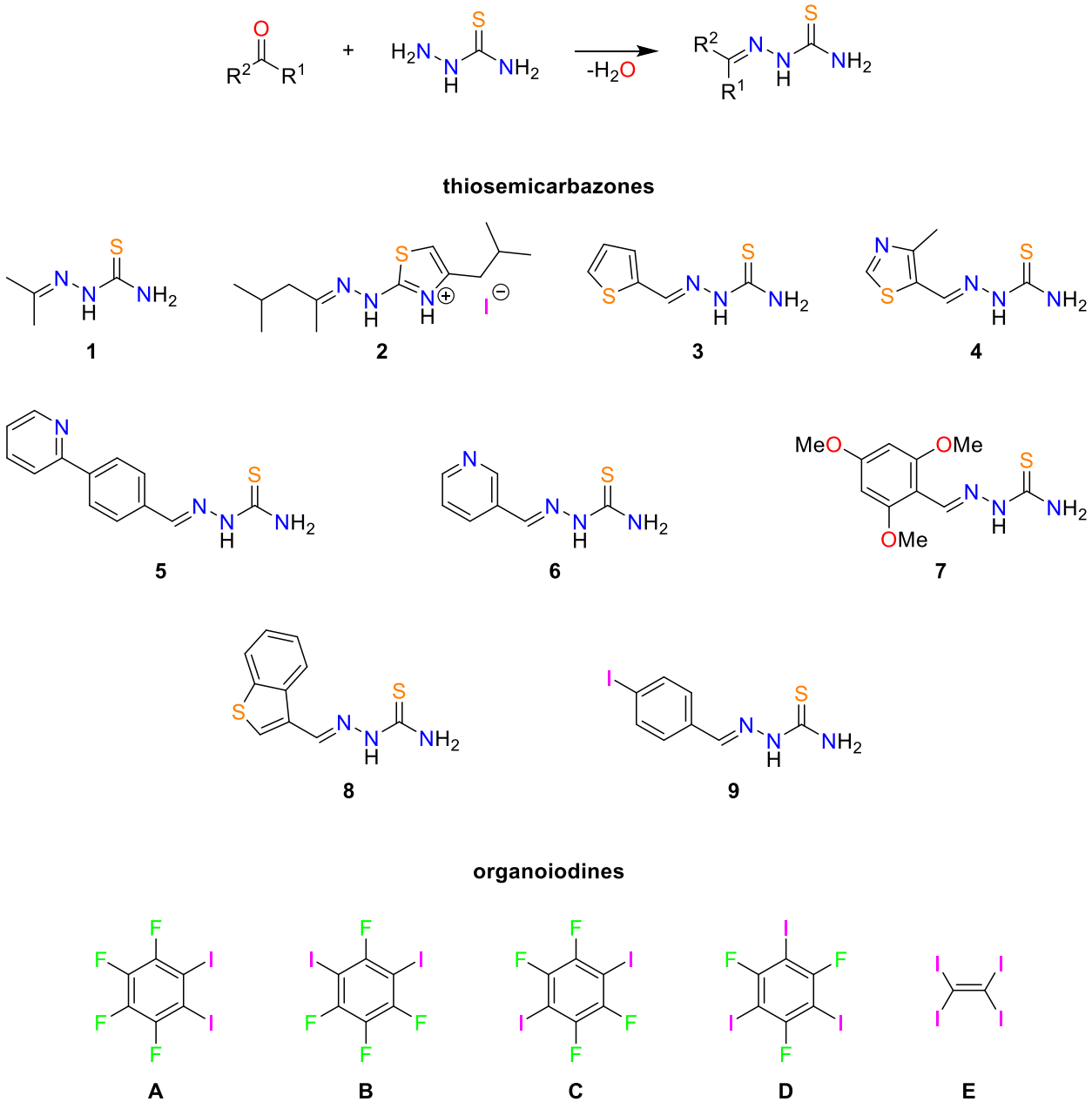

Scheme 1. Scope of thiosemicarbazones synthesized and organoiodines utilized for cocrystallization

3. Results and Discussion

3.1 Synthesis and Structures

Conveniently, acetone can be utilized as the reaction solvent, as well as carbonyl source, to yield 2-(1-methylethylidene)hydrazinecarbothiourea, **1**. Slow evaporation of these acetone solutions with organoiodines 1,2-, 1,3- and 1,4-diiodotetrafluorobenzene (**A**–**C**), 1,3,5-trifluoro-2,4,6-triiodobenzene (**D**), and tetraiodoethylene (**E**)

resulted in cocrystals for structural characterization (Figure 1). The three isomers of diiodotetrafluorobenzene each provide 1:1 cocrystals. In each case, dimers of thiourea molecules are formed through N-H···S hydrogen bonding. These dimers are connected through I···S halogen bonds, where the long-range packing motif varies based on the diiodotetrafluorobenzene isomers. In **1A**, thiourea H-bonded dimers are doubly bridged by 1,2-diiodo-3,4,5,6-tetrafluorobenzene (**A**) to form infinite chains in the [1 1 1] direction. The plane of the hydrogen bonding dimer is approximately perpendicular to the plane of molecules of **A**. The structure of **1B** contains two unique molecules of **1** and two unique molecules of 1,3-diiodo-2,4,5,6-tetrafluorobenzene (**B**), contributing to a more complex halogen bonding pattern. The formation of a thiourea hydrogen bonding dimer is still observed, with a C–I···S halogen bond occurring to each sulfur atom of the dimer, forming a basic building block of the dimer and two organoiodine molecules. In contrast to all the other cocrystals of **1**, the second C–I bond of each diiodotetrafluorobenzene molecule does not link to the next dimer through C–I···S halogen bonding. In 1B, one of these C–I iodine atoms links to the next unit through C–I···I halogen bonding, while the C–I iodine atom at the other end of the building block links to the next building block via a bifurcated set of C–I···I and C–I···S halogen bonds. This combination of interactions forms a two-dimensional sheet-like motif. While the arrangement of two C–I···S halogen bonds around each sulfur atom in **1C** appears similar to those of **1A**, the *para* geometry of the iodine atoms in 1,4-diiodo-2,3,5,6-tetrafluorobenzene (**C**) results in an entirely different long-range packing motif. Sheets of edge-sharing rectangles are formed via the I···S interactions, with thiourea hydrogen bonding dimers occupying the corners of the rectangular substructure, and molecules of **C** spanning the edges (Figure SI16). The molecules of **1** extend above and below the plane of the rectangle and interject into the center of the adjacent rectangles. Cocrystal **1D** provides an example of ribbons formed via thiourea hydrogen bonding with **1**, where ribbons propagate along the *c* axis and are formed through the cooperation of hydrogen atoms from both the primary and secondary nitrogen atoms to form asymmetric dimers. Neighboring ribbons are connected along the *b* axis through C–I···S halogen bonding. The third iodine atom of the 1,3,5-trifluoro-2,4,6-triiodobenzene (**D**) then provides halogen bonding connectivity along the *a* axis by C–I···I halogen bonding. The reaction of tetraiodoethylene (**E**) produced a mixture of two cocrystalline products. The first cocrystal, **1E**, the product of the expected addition of acetone to thiosemicarbazide, includes two molecules of **1** and one molecule of **E** in the asymmetric unit and represents the only 2:1 cocrystal of the acetone series. Thiourea dimers are connected through C–I···S halogen bonds involving *trans* iodine atoms of each molecule of **E**, forming chains. This is a common halogen bonding pattern for **E**.[33–35] The second product results from the

formal addition of one equivalent of thiosemicarbazide and four equivalents of acetone. This formation of this unexpected reaction product has not previously been reported in the literature and is likely facilitated by the iodine produced from the in-situ decomposition of **E**. Our group has previously reported bond-forming reactions facilitated by similar TIE decomposition.[36] Halogen bonds between each C–I iodine atom and an iodide anion form sheets in the *ab* plane (Figure SI17). The primary interactions to **2** include an S···I chalcogen bond to an iodine atom of **E**, as well as a pair of hydrogen bonds between both N–H hydrogen atoms in **2** and the iodide anion. It is these interactions to **2** which connect the TIE/iodide sheets in the *a* direction to form a long-range three-dimensional framework.

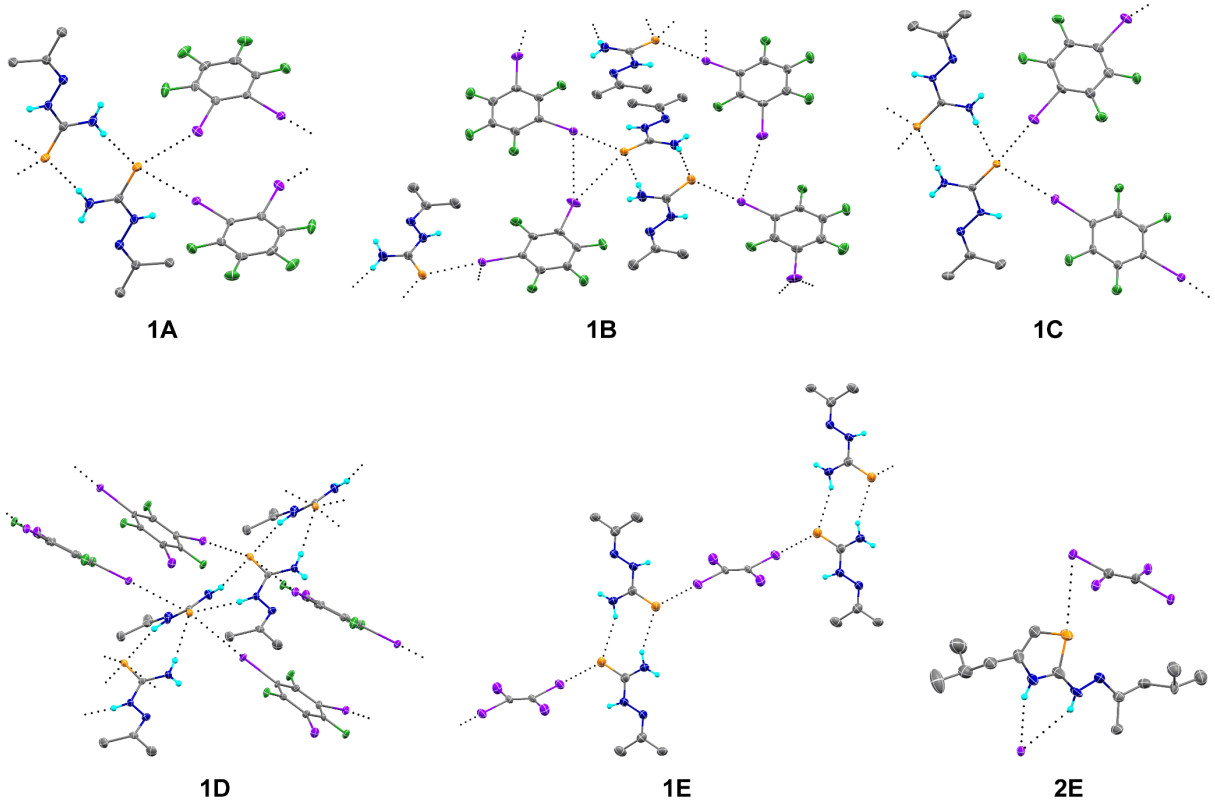

Figure 1. Halogen and hydrogen bonding in **1A**–**2E**. Intermolecular interactions are shown as dotted lines. Hydrogen atoms, except those bound to nitrogen atoms, are omitted for clarity. Atomic displacement ellipsoids are shown at the 50% probability level.

The thiosemicarbazones 2-(2-thienylmethylene)hydrazinecarbothiourea (**3**) and 2-((4-methyl-5-thiazoyl)methylene)hydrazinecarbothiourea (**4**), both of which have been previously reported in the literature,[37, 38] provide the opportunity to study the influence of additional sulfur atom-containing heterocyclic components on the resulting cocrystalline structure (Figure 2). Cocrystal **3C**, obtained by the in-situ reaction of thiosemicarbazide,

2-thiophenecarboxaldehyde, and 1,4-diiodotetrafluorobenzene (**C**) yields a 2:3 cocrystal. Hydrogen bonding dimers are observed between molecules of **3**, in this case involving the sulfur atom and the secondary N–H hydrogen atom. Each sulfur atom acts as a halogen bond acceptor in a pair of bifurcated halogen C–I···S halogen bonds. An additional C–I···S halogen bond occurs to the thiophene sulfur atom. There are one- and one-half unique molecules of **C** within the asymmetric unit, resulting in two molecules of **C** which link thiophene sulfur atoms to thione sulfur atoms, with the third full molecule of **C** linking two thione sulfur atoms. This combination of halogen bonding interactions contributes to the formation of chains along the *c* axis. The addition of a nitrogen atom within the pendant heterocycle, along with a methyl group, in **4** results in significantly different halogen bonding behavior compared to **3**. Formed from the in-situ reaction of thiosemicarbazide, 4-methyl-5-thiazolecarboxaldehyde, and the appropriate diiodotetrafluorobenzene, cocrystals **4A** and **4C** do not display halogen bonding to the heterocyclic sulfur atom. In **4A**, a 2:1 thiosemicarbazone:diiodotetrafluorobenzene cocrystal, a chain-like substructure is formed, propagating along the *b* axis by a combination of N–H···S hydrogen bonding. Here, the thione sulfur atom acts as the hydrogen bond acceptor, and both the primary and secondary N–H hydrogen atoms act as hydrogen bond donors. With the heterocyclic sulfur atom not participating in significant intermolecular interactions, it is the heterocyclic N–H that acts as a hydrogen bond donor to the thione sulfur atom of a neighboring chain, serving to link chains along the *c* axis and form hydrogen-bonded sheets of **4**. A C–I···S halogen bond links one of the iodine atoms of each molecule of **A** to the thione sulfur atom of one of the unique molecules of **4**, as decorations to the hydrogen-bonded sheets, with the second iodine atom not involved in any significant halogen bonding interactions. **4C**, which is again a 2:1 thiosemicarbazone:diiodotetrafluorobenzene cocrystal, displays coplanar thiourea dimers involving the thione sulfur atom and a primary N–H hydrogen atom, similar to those observed in the cocrystals involving **1**. The dimers are fused into chains by the continuation of N-H···S interactions, this time between the secondary N-H hydrogen atom and the thione sulfur atom (S···N = 3.632(3) Å). A weak C–H···S interaction (S···C = 3.707(4) Å), similar in length to the N–H···S hydrogen bond, is also observed from the same sulfur atom and the methine C–H which is β to the secondary nitrogen atom. These chains of dimers are linked to one another into sheets by C–I···N halogen bonding, with the heterocyclic nitrogen atom acting as the halogen bond acceptor. Unlike the previous cocrystals in this study, here the thione sulfur atom does not participate in any halogen bonding interactions and is wholly occupied by hydrogen bonding. As in **4A**, the heterocyclic sulfur atom in **4C** also does not participate in intermolecular interactions to extend the structure.

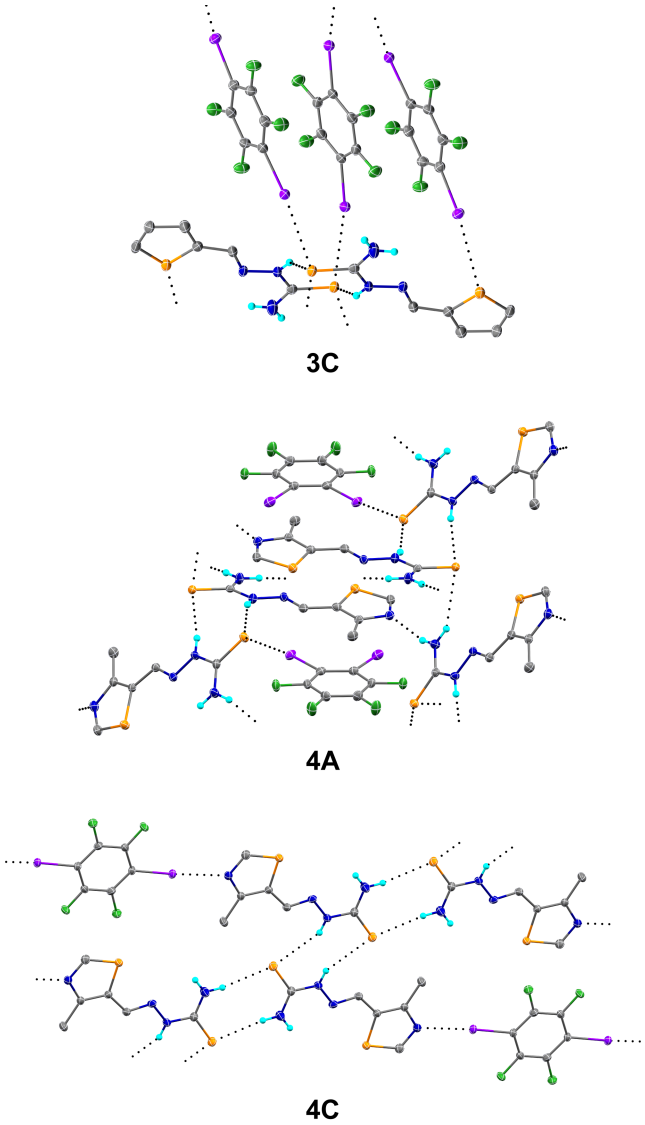

Figure 2. Halogen and hydrogen bonding in **3C**, **4A**, and **4C**. Intermolecular interactions are shown as dotted lines. Hydrogen atoms, except those bound to nitrogen atoms, are omitted for clarity. Atomic displacement ellipsoids are shown at the 50% probability level.

Both containing pyridine functionality, the semicarbazones 2-((4-(3-pyridyl)phenyl)methylene)hydrazinecarbothiourea (**5**) and 2-(3-pyridinylmethylene)hydrazinecarbothiourea (**6**), both of which have long been known in the literature, provide further examples of the role of additional hydrogen or halogen bond acceptors beyond the thiourea in the resulting crystal packing (Figure 3).[39, 40] The in situ reaction of 4-(2-pyridinyl)benzaldehyde, thiosemicarbazide, and 1,4-diiodotetrafluorobenzene (**C**) results in the 2:1 semicarbazone:1,4-diiodotetrafluorobenzene cocrystal. In **5C**, the thiourea dimer is formed through a pair of N–H···S hydrogen bonds involving the secondary N–H hydrogen atom. These dimers are then linked to one another

through C–I···S halogen bonding into the halogen bonding chain substructure propagating in the [1 1 0] direction. The pyridine nitrogen atom acts as a hydrogen bond acceptor to a hydrogen atom of the primary NH_2, thus forming a hydrogen bonding chain substructure in the *c* direction and creating the two-dimensional cooperative framework. The chain substructures that connect into the sheets are rotated by approximately 80° to one another. Although **6** differs from **5** in the position of the pyridine nitrogen atom relative to the thiosemicarbazone functionality, as well as the lack of the additional six-membered ring, a similar tendency of cooperative hydrogen bonding and halogen bonding is observed in **6C**, formed by the in-situ reaction of 3-pyridinecarboxaldehyde, thiosemicarbazide, and **C**. Again a 2:1 cocrystal, the thiourea dimers are formed between the thione sulfur atoms and the secondary N–H hydrogen atoms, just as in **5C**. The pyridine nitrogen atom functions as a hydrogen bond acceptor to a hydrogen atom of the primary nitrogen atom, forming double-stranded chains propagating in the [-1 1 0] direction (Figure SI18). Neighboring double-stranded chains in the [1 1 0] direction stack into sheets via C–I···S halogen bonding.

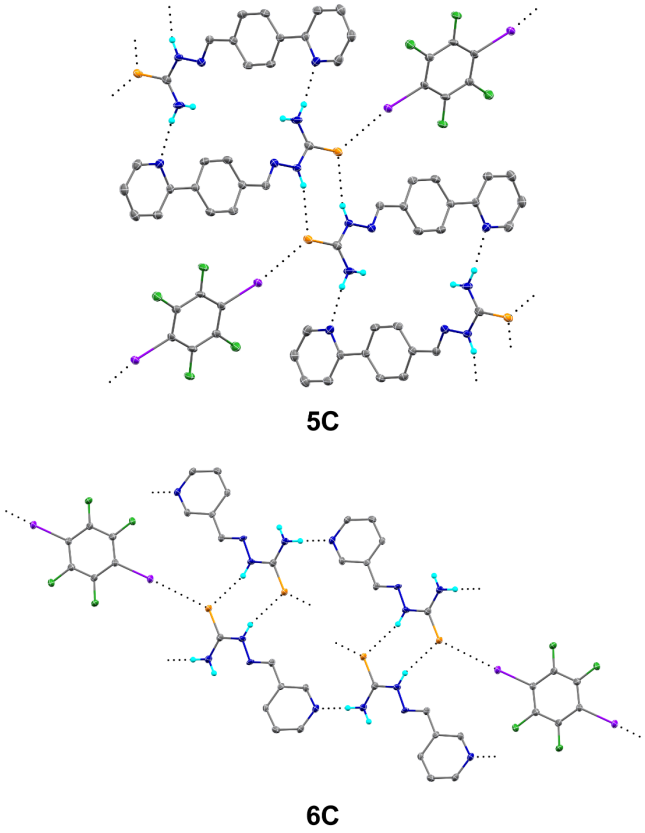

Figure 3. Halogen and hydrogen bonding in **5C** and **6C**. Intermolecular interactions are shown as dotted lines. Hydrogen atoms, except those bound to nitrogen atoms, are omitted for clarity. Atomic displacement ellipsoids are shown at the 50% probability level.

Representing the only oxygen atom-containing thiosemicarbazone in this study, **7** is formed from the reaction of thiosemicarbazide with 2,4,6-trimethoxybenzaldehyde (Figure 4 & SI19). This compound has been previously reported in the literature, but no cocrystalline structures incorporating it have been reported.[41] By converting the benzaldehyde addition to thiosemicarbazide in situ in the presence of 1,4-diiodotetrafluorobenzene (**C**), the 2:3 thiosemicarbazone:1,4-diiodotetrafluorobenzene cocrystal **7C** was obtained. The crystalline packing in this structure is dominated by N–H···S hydrogen bonding, with the sulfur atom participating in a pair of hydrogen bonds resulting in chain formation along the *c* axis. Neighboring chains of hydrogen-bonded molecules are linked in the *a* direction through a C–I···S halogen bond to one side of an organoiodine molecule of C, and a weak S···I chalcogen bond to the other side of the same molecule of C. The third stoichiometric equivalent of C in the cocrystal serves to reinforce the packing in the *b* direction by linking molecules of C through C–I···I halogen bonds, extending the cooperative hydrogen-halogen-chalcogen bonding network to be three dimensional.

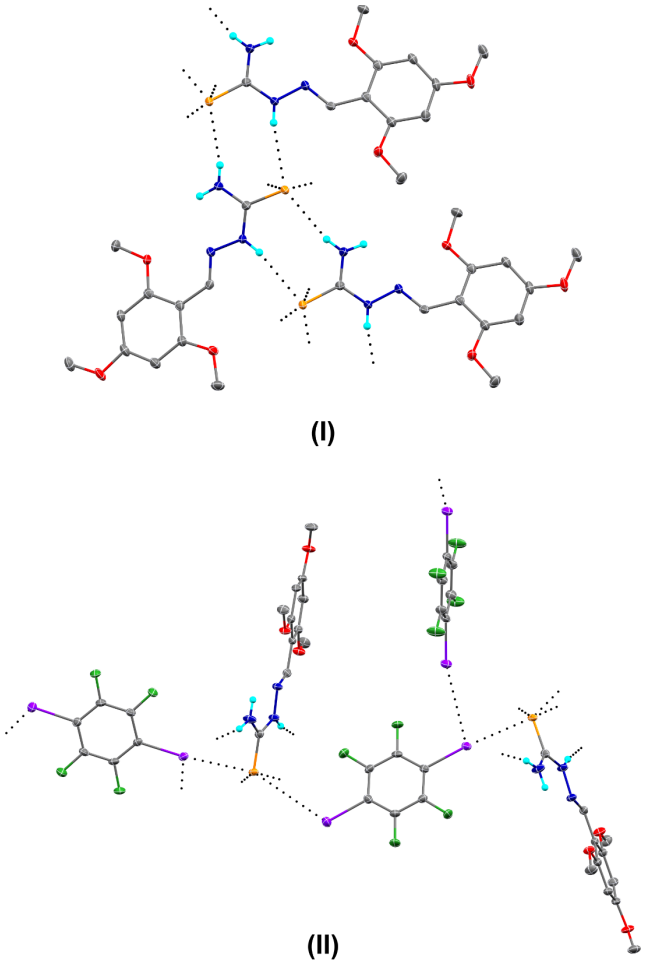

Figure 4. Hydrogen (**I**) and halogen (**II**) bonding in **7C**. Intermolecular interactions are shown as dotted lines. Hydrogen atoms, except those bound to nitrogen atoms, are omitted for clarity. Atomic displacement ellipsoids are shown at the 50% probability level.

Despite the presence of the nitrogen, sulfur, and iodide atoms outside of the thiosemicarbazone, all attempts to isolate cocrystals of 2-(benzo[*b*]thien-3-ylmethylene)hydrazinecarbothiourea (**8**) and 2-((4-iodophenyl)methylene)hydrazinecarbothiourea (**9**) with halogen bond donors were unsuccessful (Figure 5). The synthesis of each of these compounds has been previously reported, but the solid-state structures have not.[42–44] In contrast, the sulfur atom of the pendant benzo[*b*]thiophene group in **8** does not significantly contribute to the hydrogen bonding pattern. Alternating pairs of N–H···S hydrogen bonds form ribbons in the [1 0 1] direction, with the benzo[*b*]thiophene groups alternating sides as the chain propagates. An N–H···S hydrogen bond involving the second hydrogen atom of the primary nitrogen NH_2 links adjacent chains. Finally, the structure of **9** features a pendant C–I bond, which, perhaps surprisingly in the context of the above cocrystals, does not participate in any

significant halogen bonding interactions to the thione sulfur atom. Thiourea hydrogen bonding contributes to the formation of ribbons propagating in the *c* direction. The iodine atoms, which are on the outside edges of these ribbons, consolidate the packing of adjacent ribbons through a C–I···π interaction (3.4559(13) Å). This interaction places alternating layers of chains along the *c* axis roughly perpendicular to one another.

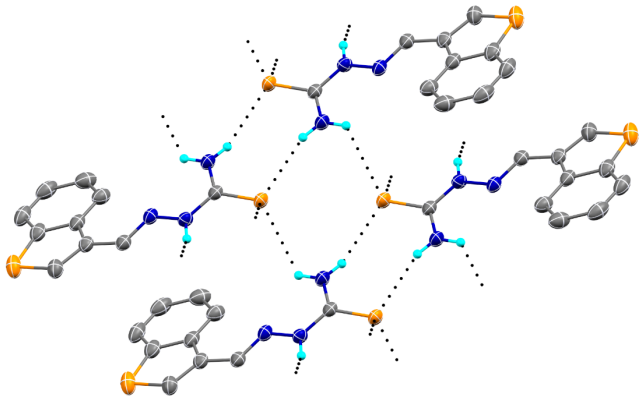

8

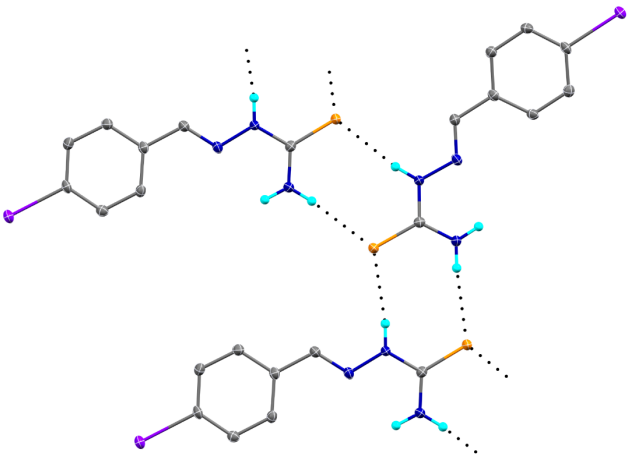

9

Figure 5. Halogen and hydrogen bonding in **8** and **9**. Intermolecular interactions are shown as dotted lines. Hydrogen atoms, except those bound to nitrogen atoms, are omitted for clarity. Atomic displacement ellipsoids are shown at the 50% probability level.

3.2 Structural Trends and Cooperative Tendencies

As demonstrated by this series of structures, thioamide dimerization is the prevailing hydrogen-bonding motif observed in thiosemicarbazone-containing molecules. Dimerization is possibly utilizing either the terminal, primary NH_2 group or the secondary NH. A search of the Cambridge Structural Database for organic-only thiosemicarbazone dimers reveals nearly an even split between these two dimerization modes, with 206 and 202

structures deposited with dimerization involving the primary and secondary nitrogen atoms respectively.[45] A similar ratio is observed in this study. The structure of **1** has been previously published, where the primary dimerization occurs through the primary nitrogen atom, with dimers combining into ribbons via weaker interactions involving the secondary nitrogen atom.[46] In adding an organoiodine, halogen bonding serves as the primary interaction for consolidating the packing of the thioamide dimers in four of the five structures in this study. The structure of **3** has also been previously reported in the literature, again with primary dimerization through the primary nitrogen with an extension of the packing through interaction to the secondary nitrogen.[47] Halogen bonding in **3C** overrides the hydrogen bonding interaction to the secondary nitrogen, with primary 2-dimensional packing driven by I···S halogen bonding. This trend holds across the series of halogen bonding cocrystals in this study. Hydrogen bonding thioamide dimerization dominates, with extension into 2- or 3-dimensional packing often provided by halogen bonding. The shortening of one interaction type is also often accompanied by a lengthening of the other. For example, in **6C**, which shows the shortest N···S distance (3.343(5) Å), also displays a relatively long C–I···S distance (3.4455(14) Å). An exception to this is observed in **4A**, in which both the hydrogen and halogen bonding distances are relatively long (>3.5 Å). In this structure, the thioamide dimerization is out-of-plane with respect to the thiosemicarbazone plane, likely influenced by both the methyl substitution, as well as the pendant nature of the halogen bonding. Other interaction types, such as C–S···I chalcogen bonding and C–I···I halogen bonding are less frequently observed.

Table 4. Selected intermolecular hydrogen and halogen bond parameters (Å, °)

Compound ID	N–H···S	C–I···S	C–S···I	C–I···N	C–I···I	N–H···I	N–H···N
1A	3.4608(17) 172.6(19)	3.2371(5) 168.70(5)	—	—	—	—	—
1B	3.430(7) 175(13)	3.131(2) 177.2(2)	—	—	—	—	—
1C	3.382(7) 169(7)	3.2183(17) 174.96(14)	—	—	—	—	—
1D	3.347(7) 167(12)	3.327(2) 171.9(2)	—	—	3.8507(7) 161.7(2)	—	—
1E	3.470(11) 154(6)	3.197(3) 177.7(3)	—	—	—	—	—
2E	—	—	3.627(3) 71.08(19)	—	3.5746(10) 177.1(2)	3.505(7) 143(11)	—
3C	3.479(4) 142(4)	3.2719(11) 161.52(10)	—	—	—	—	—
4A	3.5017(13) 162(2)	3.5815(5) 170.71(6)	—	—	—	—	3.072(2) 161(2)

4C	3.469(4) 171(5)	—	—	2.844(2) 176.07(12)	—	—	—
5C	3.432(3) 165(3)	3.1890(9) 171.51(8)	—	—	—	—	2.950(4) 163(3)
6C	3.343(5) 160(7)	3.4455(14) 162.94(19)	—	—	—	—	2.884(7) 165(8)
7C	3.489(2) 167(2)	3.1949(6) 168.89(6)	—	—	—	—	—
8	3.354(2) 162(2)	—	—	—	—	—	—
9	3.3481(16) 168(2)	—	—	—	—	—	—

Note: In the event of multiple interactions of a given type, the one with the shortest distance is tabulated. When the contact involves a hydrogen atom (X—H···Y), the distance is calculated as X···Y. In **1E**, only distances involving the primary **TIE** disorder component are tabulated.

4. Conclusions

This study presents the convenient in-situ reaction of thiosemicarbazide with carbonyls in the presence of organoiodines to provide hydrogen and halogen bonded cocrystals. Hydrogen bonding is observed in all structures, in the form of thioamide dimers, with further extensions into chains or ribbons due to the presence of multiple protic nitrogen atoms. The presence of halogen bond donors typically serves to extend the dimensionality of hydrogen bonding motifs through C–I···S halogen bonds. In the thiosemicarbazones with additional nitrogen or sulfur atom-containing functionality, the halogen bonding remains to the thione sulfur atom. The pendant nitrogen and/or sulfur atoms contribute to the dimensionality of further packing through hydrogen bonding. The cooperative and versatile nature of these interactions suggests rich supramolecular chemistry, suitable for further study and application to crystal design.

5. Data Availability

The crystallographic data including CIF and fcf files have been deposited into Cambridge Crystallographic Data Centre. CCDC 2117350 through 2117363 contain the crystallographic data. These data can be obtained free of charge from the Cambridge Crystallographic Data Centre via www.ccdc.cam.ac.uk/structures.

6. Acknowledgments

AJP acknowledges the United States Air Force Institute of Technology Civilian Institutions program and the Air Force Office of Scientific Research for fellowship support. The authors thank the NSF grants CHE-1560300 and CHE-2050042 for supporting this work.

7. Competing Interests

WTP is the Editor-in-Chief of the Journal of Chemical Crystallography. CDM is an Associate Editor with the Journal of Chemical Crystallography. They have been excluded from the peer review process.

References

1. Desiraju GR, Shing Ho P, Kloo L, Legon AC, Marquardt R, Metrangolo P, Politzer P, Resnati G, Rissanen K (2013) Definition of the halogen bond (IUPAC recommendations 2013). Pure Appl Chem 85:1711–1713 . https://doi.org/10.1351/PAC-REC-12-05-10

2. Parisini E, Metrangolo P, Pilati T, Resnati G, Terraneo G (2011) Halogen bonding in halocarbon-protein complexes: A structural survey. Chem Soc Rev 40:2267–2278 . https://doi.org/10.1039/c0cs00177e

3. Zhou P, Tian F, Zou J, Shang Z (2010) Rediscovery of Halogen Bonds in Protein-Ligand Complexes. Mini-Reviews Med Chem 10:309–314

4. Metrangolo P, Resnati G (2015) Topics in Current Chemistry: Halogen Bonding II. Springer International Publishing

5. Metrangolo P, Resnati G (2008) Structure and Bonding: Halogen Bonding. Springer International Publishing

6. Metrangolo P, Resnati G (2015) Topics in Current Chemistry: Halogen Bonding I. Springer International Publishing

7. Metrangolo P, Resnati G (2012) Halogen bonding: Where we are and where we are going. Cryst Growth Des 12:5835–5838 . https://doi.org/10.1021/cg301427a

8. Cavallo G, Metrangolo P, Milani R, Pilati T, Priimagi A, Resnati G, Terraneo G (2016) The halogen bond. Chem Rev 116:2478–2601 . https://doi.org/10.1021/acs.chemrev.5b00484

9. Metrangolo P, Neukirch H, Pilati T, Resnati G (2005) Halogen bonding based recognition processes: A world parallel to hydrogen bonding. Acc Chem Res 38:386–395 . https://doi.org/10.1021/ar0400995

10. Legon AC (1998) π-Electron “donor-acceptor” complexes B ⋯ ClF and the existence of the “chlorine

bond.” Chem - A Eur J 4:1890–1897 . https://doi.org/10.1002/(SICI)1521-3765(19981002)4:10<1890::AID-CHEM1890>3.0.CO;2-4

11. Corradi E, Meille S V., Messina MT, Metrangolo P, Resnati G (2000) Halogen bonding versus hydrogen bonding in driving self-assembly processes. Angew Chemie - Int Ed 39:1782–1786 . https://doi.org/10.1002/(SICI)1521-3773(20000515)39:10<1782::AID-ANIE1782>3.0.CO;2-5

12. Sakunthaladevi R, Jothi L (2021) Growth dynamics and molecular structural analysis of Dimethylketo thiosemicarbazone single crystals for frequency conversion applications - Optical and thermal characterization. J Mol Struct 1239:130463 . https://doi.org/10.1016/j.molstruc.2021.130463

13. Pavan FR, Maia PI d. S, Leite SRA, Deflon VM, Batista AA, Sato DN, Franzblau SG, Leite CQF (2010) Thiosemicarbazones, semicarbazones, dithiocarbazates and hydrazide/hydrazones: Anti - Mycobacterium tuberculosis activity and cytotoxicity. Eur J Med Chem 45:1898–1905 . https://doi.org/10.1016/j.ejmech.2010.01.028

14. Agarwal RK, Singh L, Sharma DK (2006) Synthesis, spectral, and biological properties of copper(II) complexes of thiosemicarbazones of Schiff bases derived from 4-aminoantipyrine and aromatic aldehydes. Bioinorg Chem Appl 2006:1–10 . https://doi.org/10.1155/BCA/2006/59509

15. Richardson DR, Kalinowski DS, Richardson V, Sharpe PC, Lovejoy DB, Islam M, Bernhardt P V. (2009) 2-Acetylpyridine thiosemicarbazones are potent iron chelators and antiproliferative agents: Redox activity, iron complexation and characterization of their antitumor activity. J Med Chem 52:1459–1470 . https://doi.org/10.1021/jm801585u

16. Kulandaivelu U, Chawada B, Boyapati S, Reddy AR (2014) Synthesis Antimicrobial and Anticancer Activity of 1-[(arylalkylidene)amino]-3-(4H-1,2,4-triazol-4-yl)thiourea. J Pharm Chem 1:5 . https://doi.org/10.14805/jphchem.2014.art4

17. Mohamed NA, Mohamed RR, Seoudi RS (2014) Synthesis and characterization of some novel antimicrobial thiosemicarbazone O-carboxymethyl chitosan derivatives. Int J Biol Macromol 63:163–169 . https://doi.org/10.1016/j.ijbiomac.2013.10.044

18. Sharma D, Jasinski JP, Smolinski VA, Kaur M, Paul K, Sharma R (2020) Synthesis and structure of complexes (NiII, AgI) of substituted benzaldehyde thiosemicarbazones and antitubercular activity of NiII complex. Inorganica Chim Acta 499:119187 . https://doi.org/10.1016/j.ica.2019.119187

19. Khan A, Jasinski JP, Smolenski VA, Hotchkiss EP, Kelley PT, Shalit ZA, Kaur M, Paul K, Sharma R (2018) Enhancement in anti-tubercular activity of indole based thiosemicarbazones on complexation with copper(I) and silver(I) halides: Structure elucidation, evaluation and molecular modelling. Bioorg Chem 80:303–318 . https://doi.org/10.1016/j.bioorg.2018.06.027

20. Khan A, Paul K, Singh I, Jasinski JP, Smolenski VA, Hotchkiss EP, Kelley PT, Shalit ZA, Kaur M, Banerjee S, Roy P, Sharma R (2020) Copper(i) and silver(i) complexes of anthraldehyde thiosemicarbazone: Synthesis, structure elucidation,: In vitro anti-tuberculosis/cytotoxic activity and interactions with DNA/HSA. Dalt Trans 49:17350–17367 . https://doi.org/10.1039/d0dt03104f

21. Haas KL, Franz KJ (2009) Application of metal coordination chemistry to explore and manipulate cell biology. Chem Rev 109:4921–4960 . https://doi.org/10.1021/cr900134a

22. Sun RWY, Ma DL, Wong ELM, Che CM (2007) Some uses of transition metal complexes as anti-cancer and anti-HIV agents. Dalt Trans 4884–4892 . https://doi.org/10.1039/b705079h

23. Güveli Ş, Cnar SA, Karahan Ö, Aviyente V, Ülküseven B (2016) Nickel(II)-PPh3 Complexes of S,N-Substituted Thiosemicarbazones - Structure, DFT Study, and Catalytic Efficiency. Eur J Inorg Chem 2016:538–544 . https://doi.org/10.1002/ejic.201501227

24. Castiñeiras A, Fernández-Hermida N, García-Santos I, Gómez-Rodríguez L (2012) Neutral NiII, PdII and PtII ONS-pincer complexes of 5-acetylbarbituric-4N-dimethylthiosemicarbazone: Synthesis, characterization and properties. J Chem Soc Dalt Trans 41:13486–13495 . https://doi.org/10.1039/c2dt31753b

25. Peloquin AJ, McMillen CD, Iacono ST, Pennington WT (2021) Halogen and Chalcogen Bonding Between the Triphenylphosphine Chalcogenides (Ph3P=E; E=O, S, Se) and Iodofluorobenzenes. Chempluschem 86:549–557 . https://doi.org/10.1002/cplu.202100042

26. Peloquin AJ, McCollum JM, McMillen CD, Pennington WT (2021) Halogen Bonding in Dithiane/Iodofluorobenzene Mixtures: A New Class of Hydrophobic Deep Eutectic Solvents. Angew Chemie - Int Ed 80918:22983–22989 . https://doi.org/10.1002/anie.202110520

27. Peloquin AJ, Ragusa AC, McMillen CD, Pennington WT (2021) The reaction of thiourea and 1,3-dimethylthiourea towards organoiodines: oxidative bond formation and halogen bonding. Acta Crystallogr Sect C Struct Chem 77:1–11 . https://doi.org/10.1107/s205322962100869x

28. Bruker. APEX3. Bruker AXS: Madison, WI, USA 2015.

29. CrystalClear (1999) Rigaku/MSC, The Woodlands, TX, USA.

30. Sheldrick GM (2015) Crystal structure refinement with SHELXL. Acta Crystallogr Sect C Struct Chem 71:3–8 . https://doi.org/10.1107/S2053229614024218

31. Dolomanov O V., Bourhis LJ, Gildea RJ, Howard JAK, Puschmann H (2009) OLEX2: A complete structure solution, refinement and analysis program. J Appl Crystallogr 42:339–341 . https://doi.org/10.1107/S0021889808042726

32. Bourhis LJ, Dolomanov O V., Gildea RJ, Howard JAK, Puschmann H (2015) The anatomy of a comprehensive constrained, restrained refinement program for the modern computing environment - Olex2 dissected. Acta Crystallogr Sect A 71:59–75 . https://doi.org/10.1107/S2053273314022207

33. Jay JI, Padgett CW, Walsh RDB, Hanks TW, Pennington WT (2001) Noncovalent Interactions in 2-Mercapto-1-methylimidazole Complexes with Organic Iodides. Cryst Growth Des 1:501–507 . https://doi.org/10.1021/cg015538a

34. Bats JW, Seibel A, Bock H (2016) HACWOA : 1,4,8,11-tetrathiacyclotetradecane tetraiodoethene. CSD Commun CCDC 961744 . https://doi.org/10.5517/ccdc.csd.cc118s03

35. Arman HD, Gieseking RL, Hanks TW, Pennington WT (2010) Complementary halogen and hydrogen bonding: Sulfur···iodine interactions and thioamide ribbons. Chem Commun 46:1854–1856 . https://doi.org/10.1039/b925710a

36. Peloquin AJ, Ragusa AC, McMillen CD, Pennington WT (2021) The reaction of thiourea and 1,3-

dimethylthiourea towards organoiodines: oxidative bond formation and halogen bonding. Acta Crystallogr Sect C Struct Chem 77:599–609 . https://doi.org/10.1107/s205322962100869x

37. Campaigne E, Thompson RL, Werthac JEV (1959) Some Heterocyclic Aldehyde Thiosemicarbazones Possessing Anti-viral Activity. J Med Pharm Chem 1:577–599 . https://doi.org/10.1021/jm50007a003

38. Bernstein J, Yale HL, Losee K, Holsing M, Martins J, Lott WA (1951) The Chemotherapy of Experimental Tuberculosis. III. The Synthesis of Thiosemicarbazones and Related Compounds. J Am Chem Soc 73:906–912 . https://doi.org/10.1021/ja01147a007

39. Cymerman-Craig J, Rubbo SD, Loder JW, Pierson BJ (1956) Chemical constitution and anti-tuberculous activity: Part IV. Thiosemicarbazones and related compounds. Br J Exp Pathol 37:1–4 . https://doi.org/10.1007/bf01827320

40. Gardner TS, Smith FA, Wenis E, Lee J (1951) The synthesis of compounds for the chemotherapy of tuberculosis. I. Heterocyclic thiosemicarbazide derivatives. J Org Chem 16:1121–1125

41. Somogyi L (2004) Sythesis, oxidation and dehydrogenation of cyclic N,O- and N,S-acetals. Part 1. Transformation of N,S-acetals: 3-Acyl-1,3,4-thiadiazolines. Heterocycles 63:2243–2267 . https://doi.org/10.3987/COM-04-10137

42. Ozadali K, Unsal Tan O, Yogeeswari P, Dharmarajan S, Balkan A (2014) Synthesis and antimycobacterial activities of some new thiazolylhydrazone derivatives. Bioorganic Med Chem Lett 24:1695–1697 . https://doi.org/10.1016/j.bmcl.2014.02.052

43. Campaigne E, Neiss ES (1966) Benzo[b]thiophene Derivatives. VIII. Benzo[b]thiophene-3-carboxaldehyde and Derivatives. J Heterocycl Chem 3:46–50

44. Omar AM, Ihmaid S, Habib ESE, Althagfan SS, Ahmed S, Abulkhair HS, Ahmed HEA (2020) The rational design, synthesis, and antimicrobial investigation of 2-Amino-4-Methylthiazole analogues inhibitors of GlcN-6-P synthase. Bioorg Chem 99:103781 . https://doi.org/10.1016/j.bioorg.2020.103781

45. Groom CR, Bruno IJ, Lightfoot MP, Ward SC (2016) The Cambridge structural database. Acta Crystallogr Sect B Struct Sci Cryst Eng Mater 72:171–179 . https://doi.org/10.1107/S2052520616003954

46. G. J. Palenik, D. F. Rendle WSC (1974) The crystal and molecular structures of thiosemicarbazones; an antitumor agent 5-hydroxy-2-formylpyridine thiosemicarbazone sesquihydrate and the inactive acetone thiosemicarbazone. Acta Crystallogr Sect B Struct Sci B30:2390–2395 . https://doi.org/10.1107/s0567740874007187

47. Ali NHSO, Hamid MHSA, Putra NAAMA, Adol HA, Mirza AH, Usman A, Siddique TA, Hoq MR, Karim MR (2020) Efficient eco-friendly syntheses of dithiocarbazates and thiosemicarbazones. Green Chem Lett Rev 13:129–140 . https://doi.org/10.1080/17518253.2020.1737252

Supporting Information

Synthesis of thiosemicarbazones and their organoiodine cocrystals: cooperative effects of halogen and hydrogen bonding

Andrew J. Peloquin, Arianna C. Ragusa, Hadi D. Arman, Colin D. McMillen, and William T. Pennington

Department of Chemistry, Clemson University, Clemson, South Carolina (USA)

Table of Contents

Table SI1. Bond lengths and angles of thiosemicarbazones (Å, °)

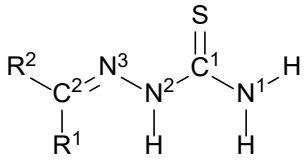

Compound ID	N^1–C^1	C^1–N^2	N^2–N^3	N^3=C^2	N^1–C^1–N^2	C^1–N^2–N^3	N^2–N^3=C^2
1A	1.327(2)	1.347(2)	1.393(3)	1.281(2)	117.2(2)	119.44(15)	115.95(15)
1B	1.326(10)	1.353(9)	1.380(9)	1.290(9)	116.8(7)	119.5(6)	116.4(7)
	1.314(11)	1.355(9)	1.388(9)	1.294(9)	117.4(7)	118.8(6)	116.0(6)
1C	1.333(8)	1.343(7)	1.392(7)	1.288(8)	116.5(5)	118.5(5)	117.0(6)
	1.332(8)	1.339(8)	1.392(6)	1.294(9)	117.7(5)	119.1(5)	116.3(6)
1D	1.340(11)	1.354(10)	1.395(10)	1.274(10)	117.1(7)	117.7(6)	116.8(6)
1E	1.314(14)	1.350(16)	1.387(17)	1.278(16)	117.4(12)	118.9(9)	116.8(9)
3C	1.320(5)	1.338(5)	1.375(4)	1.282(5)	117.4(3)	120.5(3)	113.8(3)
4A	1.325(2)	1.350(2)	1.377(2)	1.287(2)	116.96(18)	119.95(13)	114.40(14)
	1.327(2)	1.352(2)	1.383(3)	1.286(2)	117.30(19)	119.99(14)	114.83(14)
4C	1.314(6)	1.344(4)	1.376(4)	1.284(4)	117.5(3)	120.4(3)	114.4(3)
5C	1.324(4)	1.347(4)	1.381(3)	1.282(4)	117.1(3)	119.8(2)	114.5(2)
6C	1.319(8)	1.349(7)	1.373(6)	1.274(7)	118.2(5)	118.9(5)	116.8(5)
7C	1.324(3)	1.337(3)	1.387(3)	1.286(3)	117.1(2)	119.19(17)	112.56(17)
8	1.321(2)	1.345(3)	1.381(3)	1.281(3)	117.7(2)	119.07(14)	115.35(16)
9	1.320(2)	1.348(2)	1.378(2)	1.280(2)	117.46(16)	118.33(15)	116.52(15)

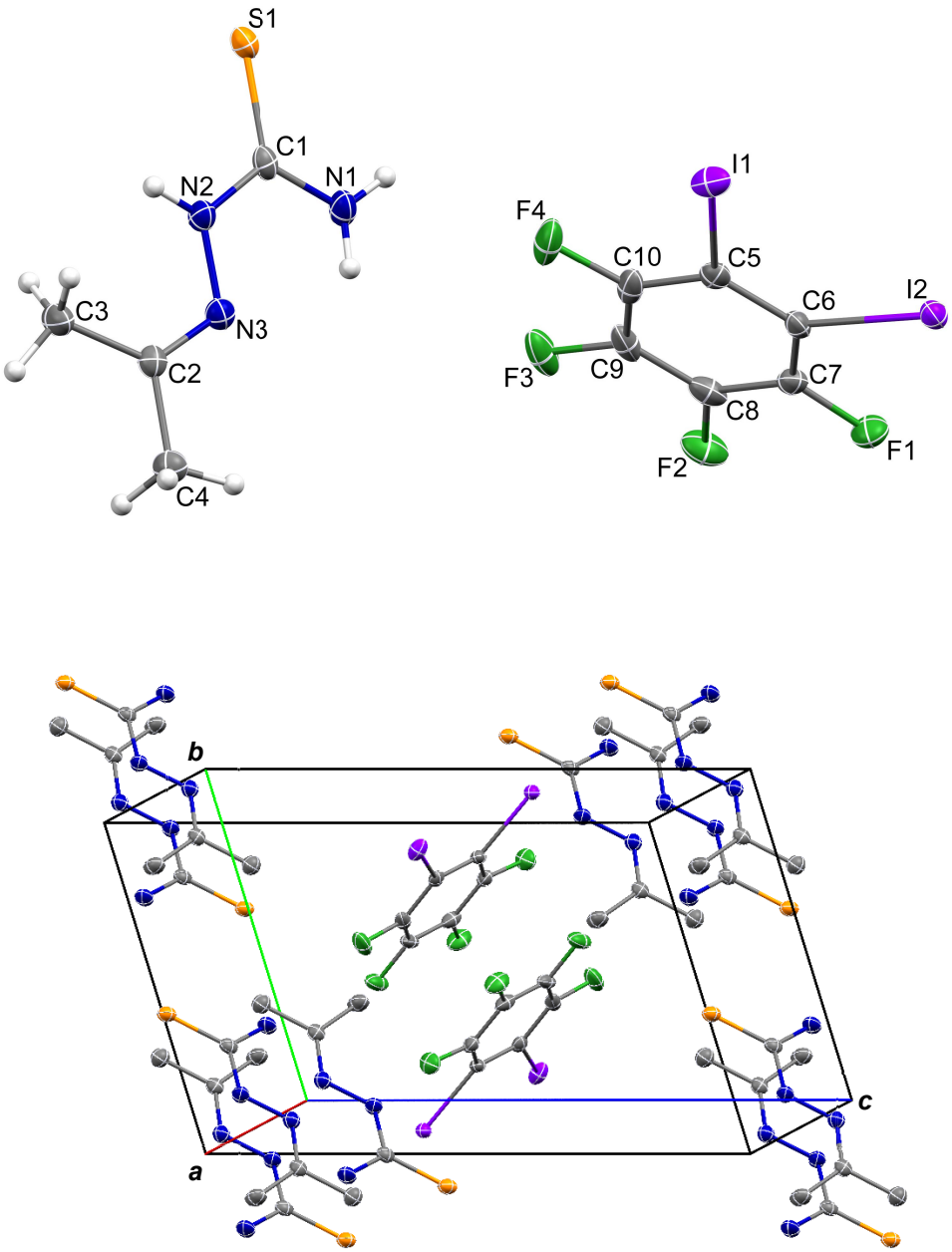

Figure SI1. Asymmetric unit (top) and unit cell packing (bottom) of **1A**. Hydrogen atoms are omitted for clarity. Atomic displacement ellipsoids are shown at the 50% probability level.

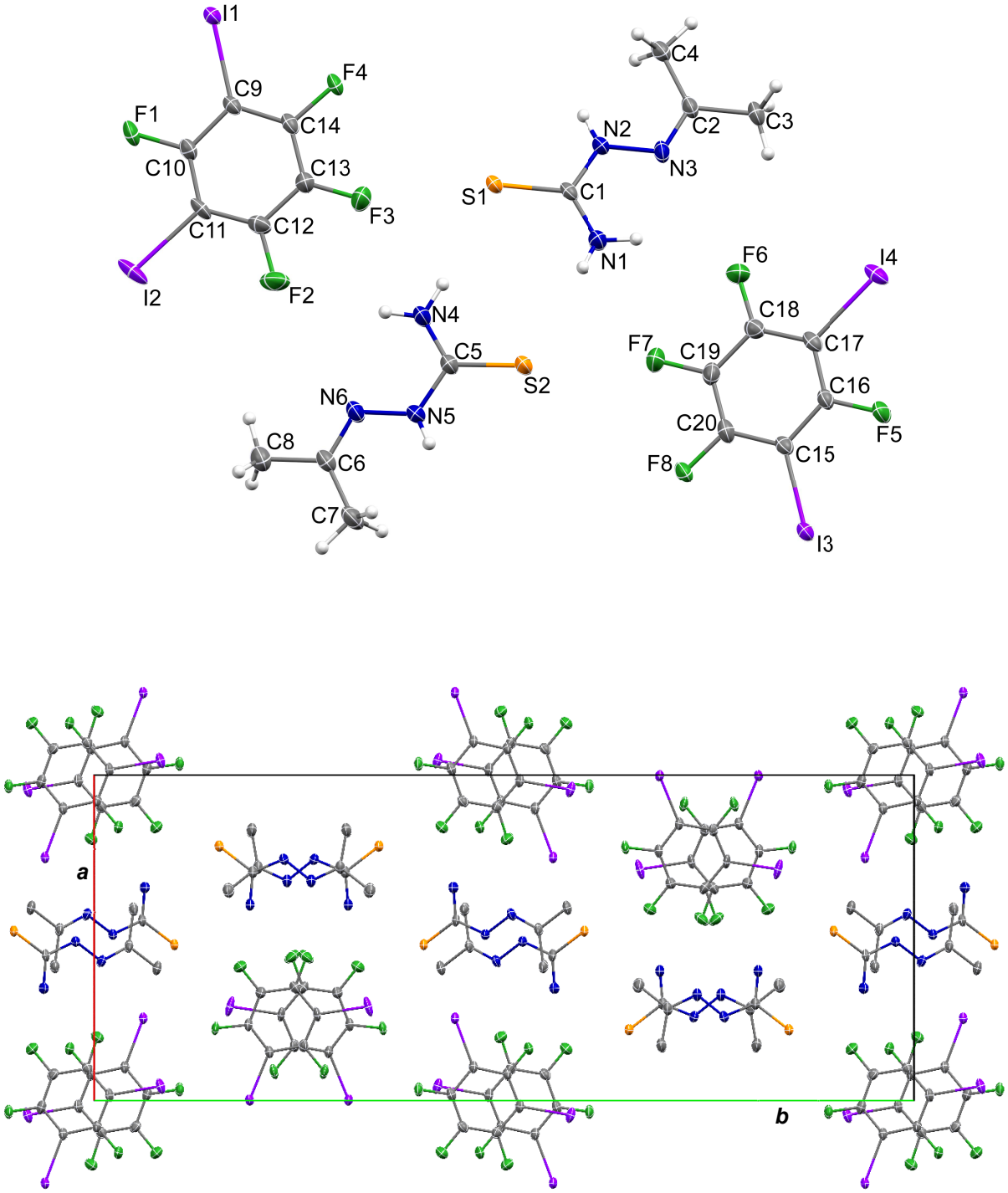

Figure SI2. Asymmetric unit (top) and unit cell packing (bottom) of **1B**. Hydrogen atoms are omitted for clarity. Atomic displacement ellipsoids are shown at the 50% probability level.

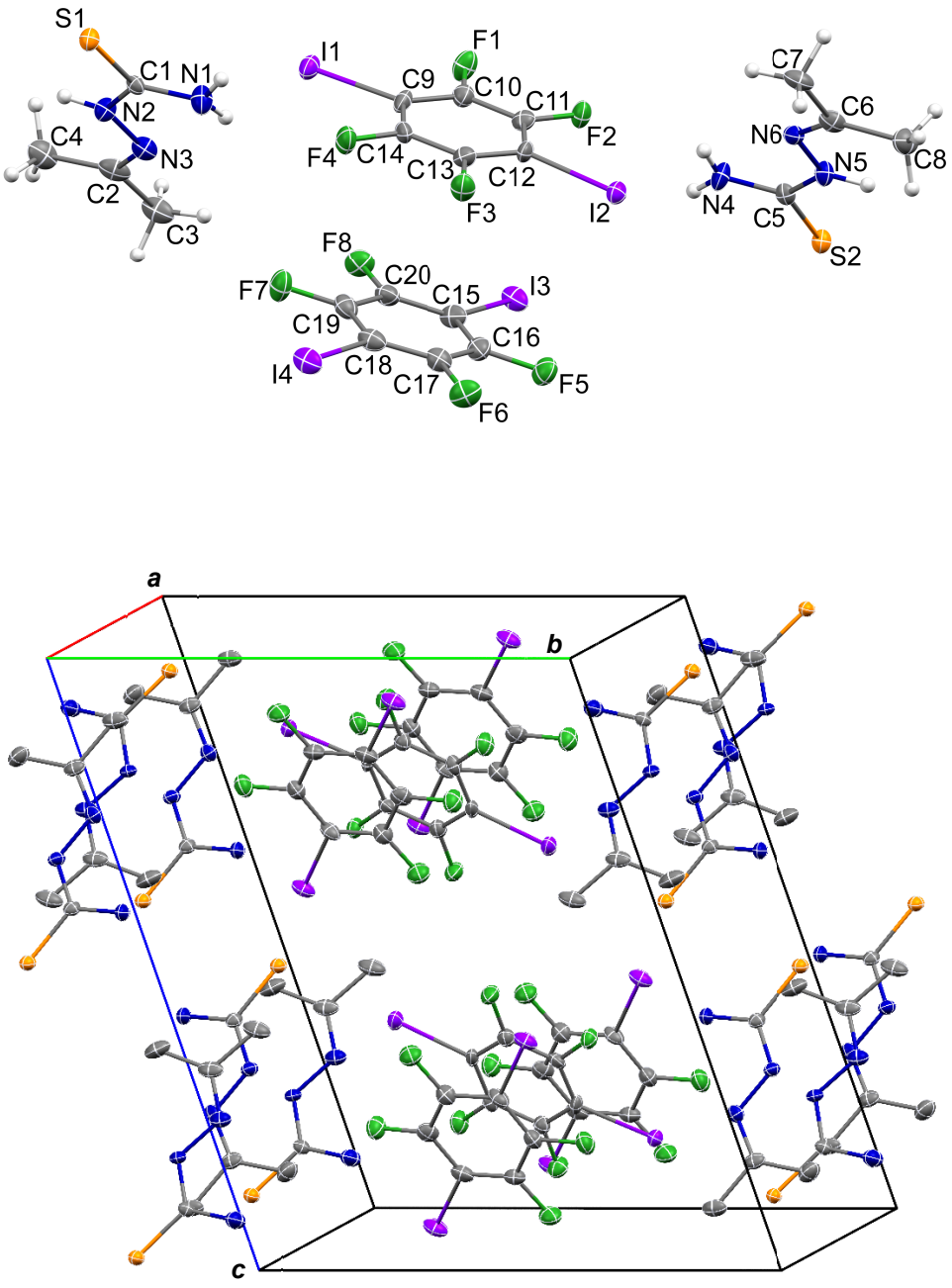

Figure SI3. Asymmetric unit (top) and unit cell packing (bottom) of **1C**. Hydrogen atoms are omitted for clarity. Atomic displacement ellipsoids are shown at the 50% probability level.

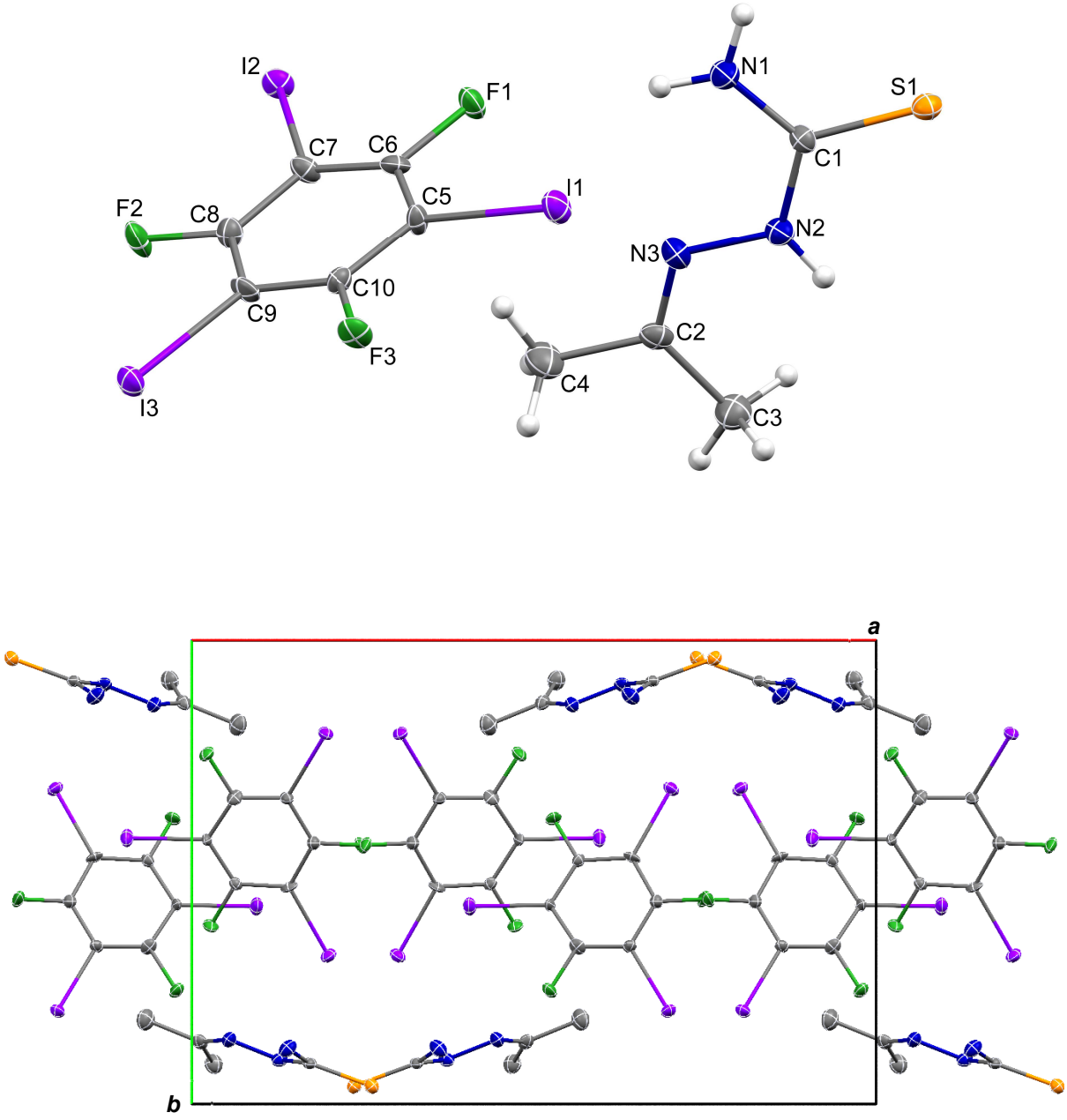

Figure SI4. Asymmetric unit (top) and unit cell packing (bottom) of **1D**. Hydrogen atoms are omitted for clarity. Atomic displacement ellipsoids are shown at the 50% probability level.

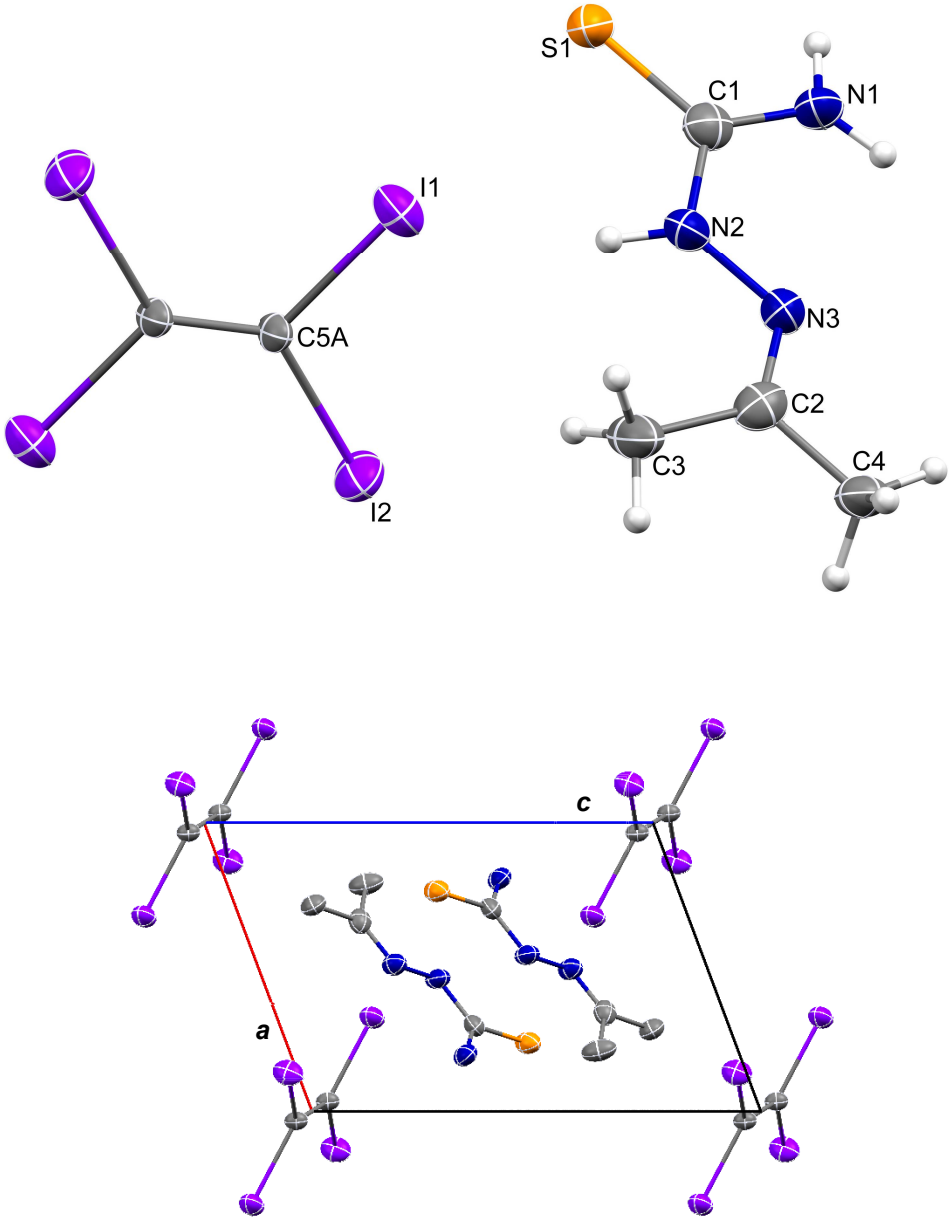

Figure SI5. Asymmetric unit (top) and unit cell packing (bottom) of **1E**. Hydrogen atoms are omitted for clarity. Atomic displacement ellipsoids are shown at the 50% probability level.

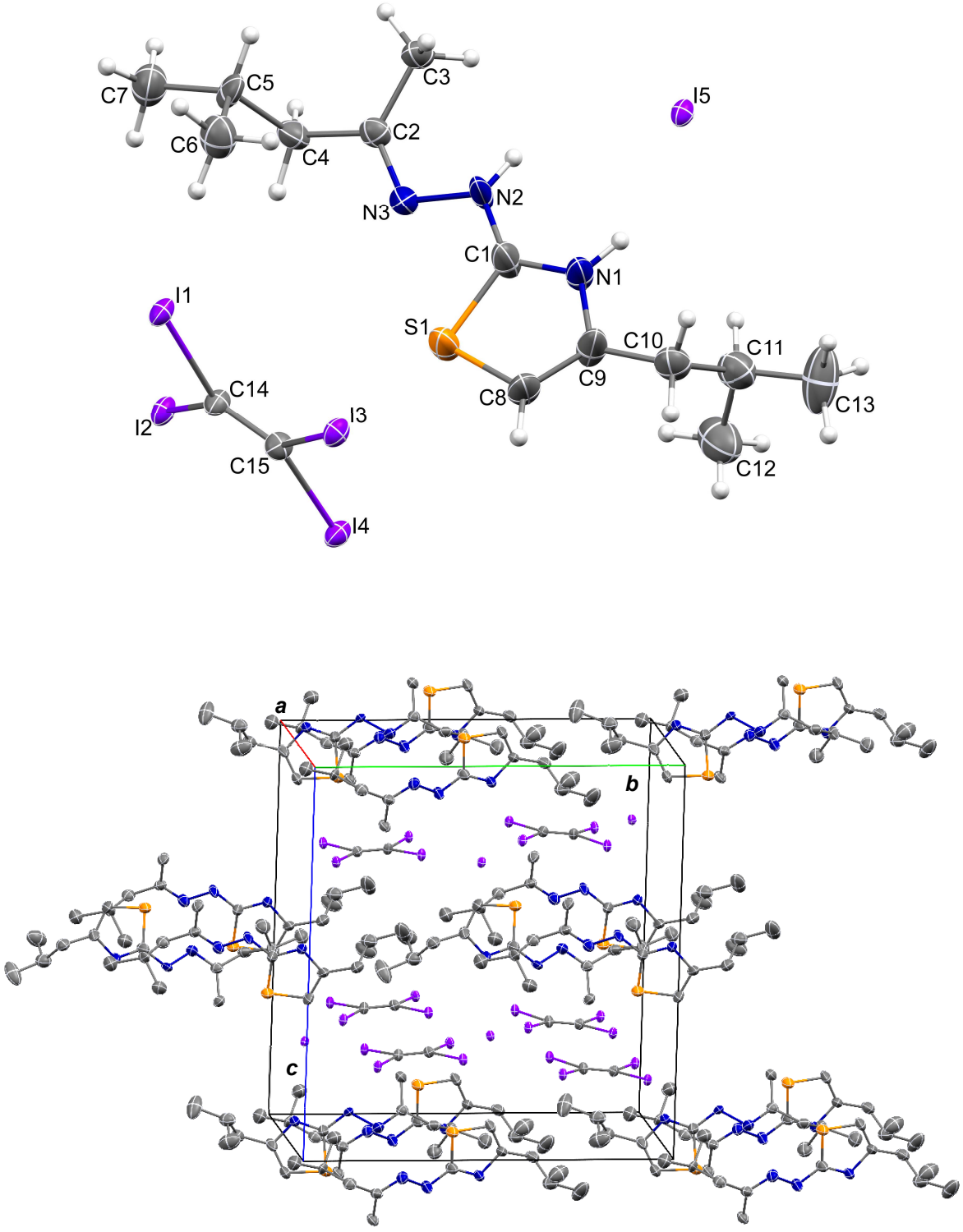

Figure SI6. Asymmetric unit (top) and unit cell packing (bottom) of **2E**. Hydrogen atoms are omitted for clarity. Atomic displacement ellipsoids are shown at the 50% probability level.

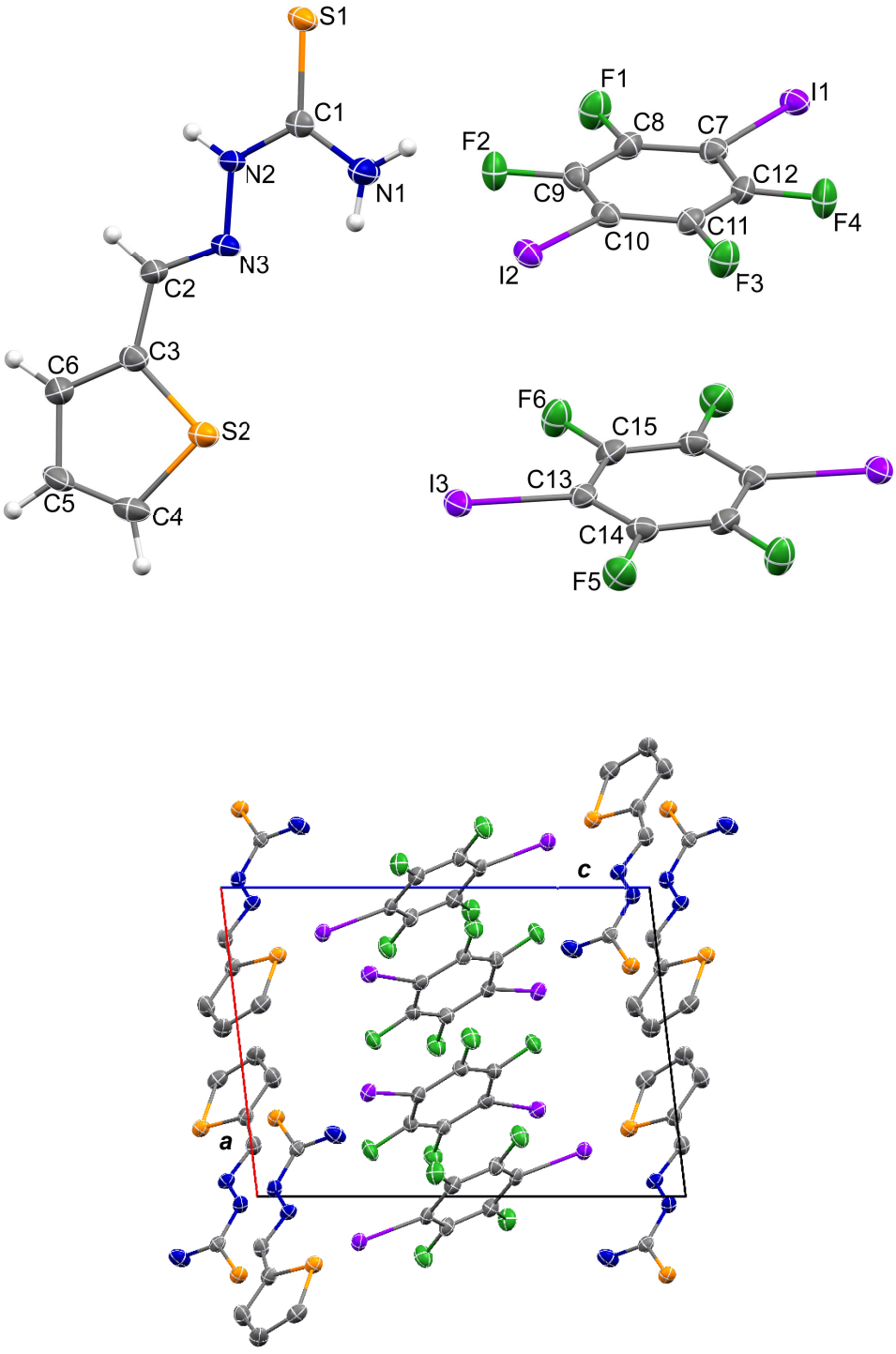

Figure SI7. Asymmetric unit (top) and unit cell packing (bottom) of **3C**. Hydrogen atoms are omitted for clarity. Atomic displacement ellipsoids are shown at the 50% probability level.

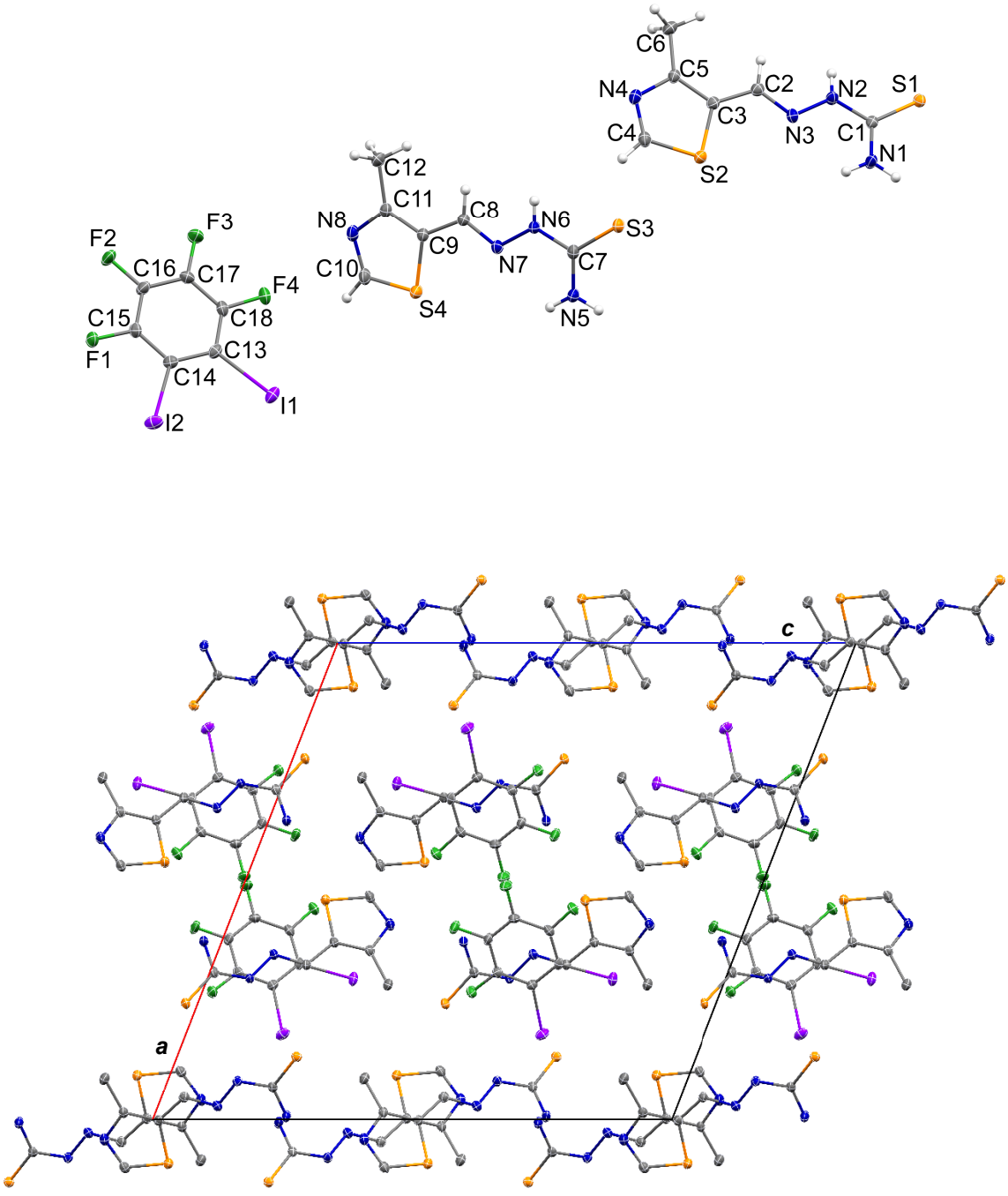

Figure SI8. Asymmetric unit (top) and unit cell packing (bottom) of **4A**. Hydrogen atoms are omitted for clarity. Atomic displacement ellipsoids are shown at the 50% probability level.

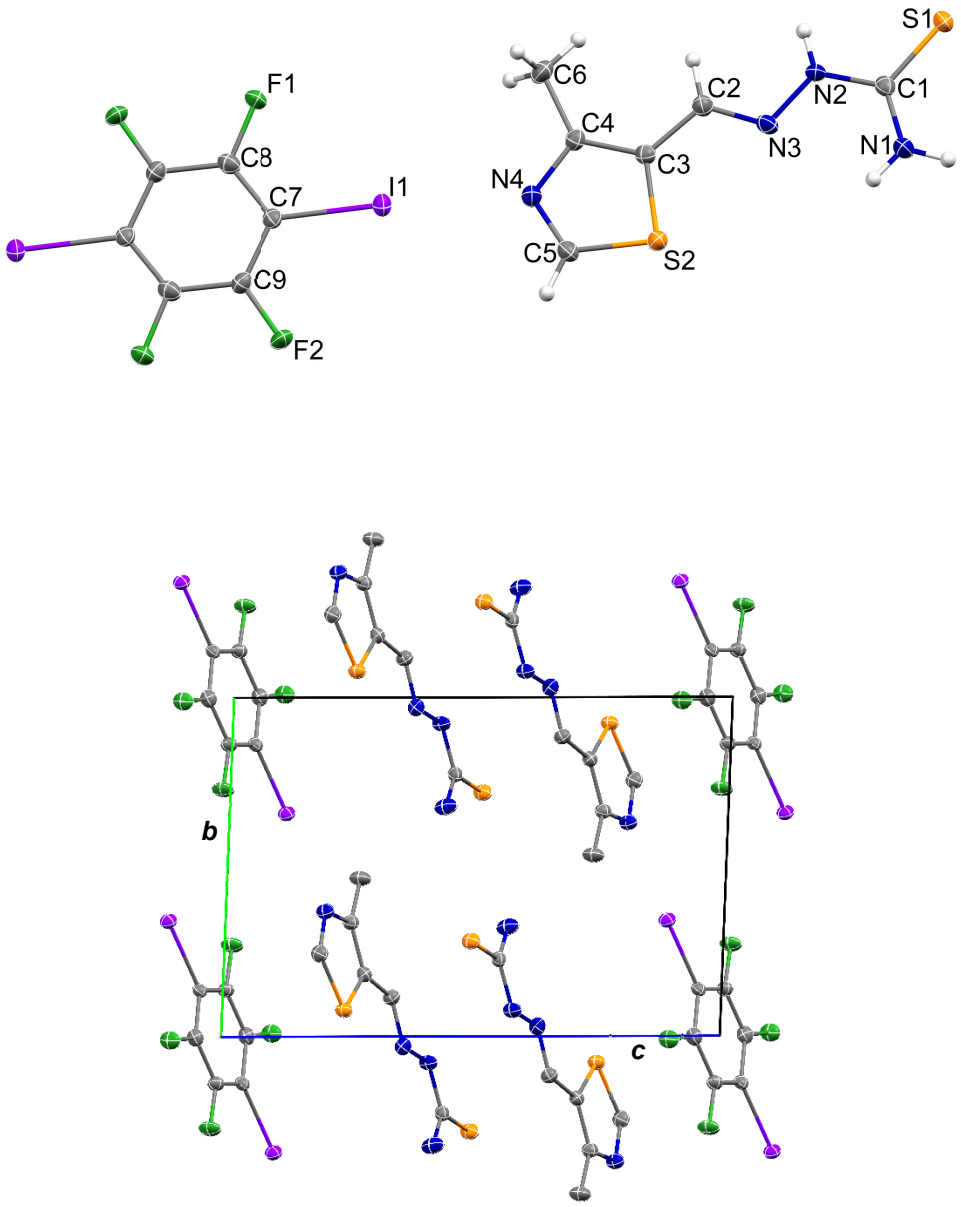

Figure SI9. Asymmetric unit (top) and unit cell packing (bottom) of **4C**. Hydrogen atoms are omitted for clarity. Atomic displacement ellipsoids are shown at the 50% probability level.

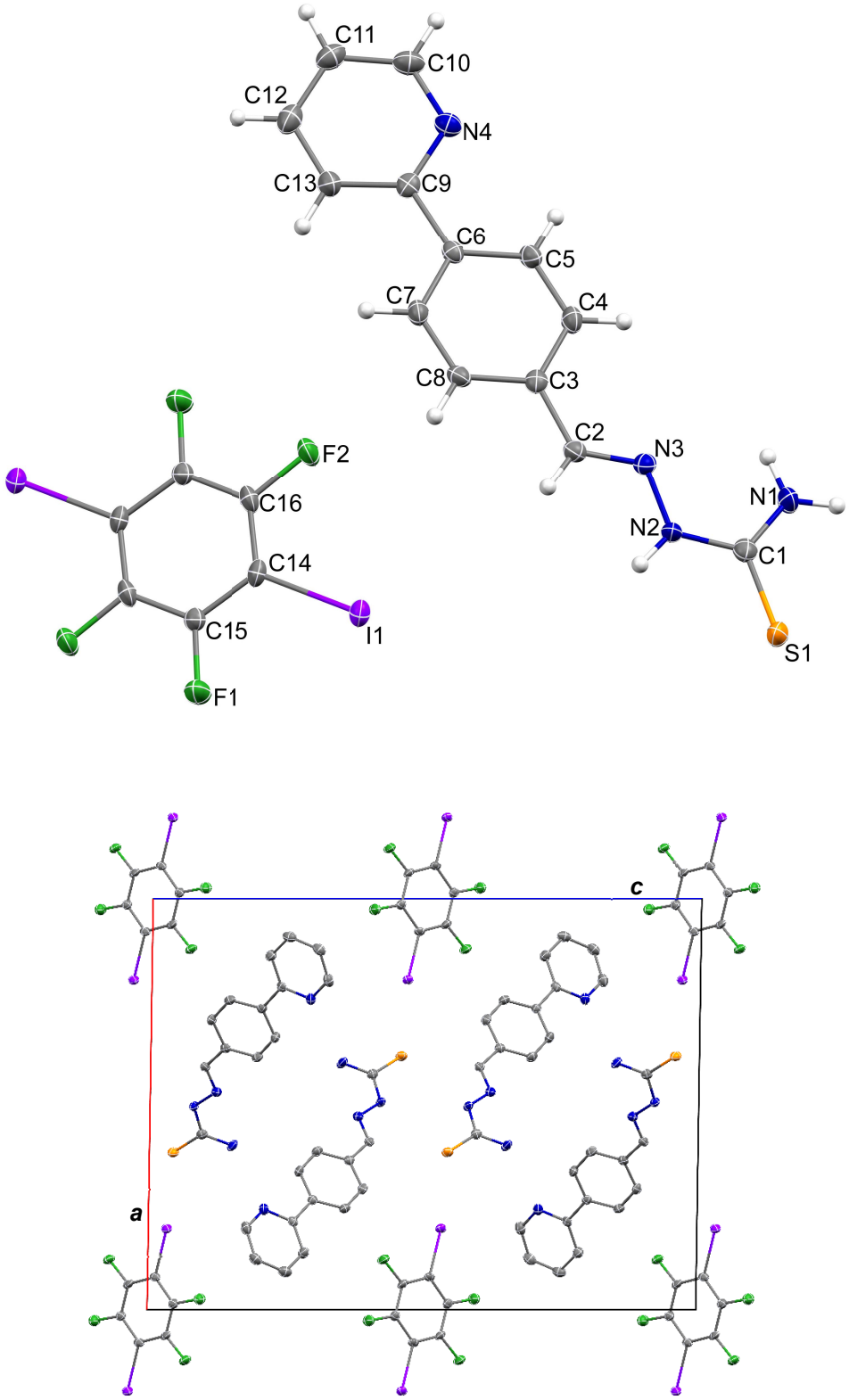

Figure SI10. Asymmetric unit (top) and unit cell packing (bottom) of **5C**. Hydrogen atoms are omitted for clarity. Atomic displacement ellipsoids are shown at the 50% probability level.

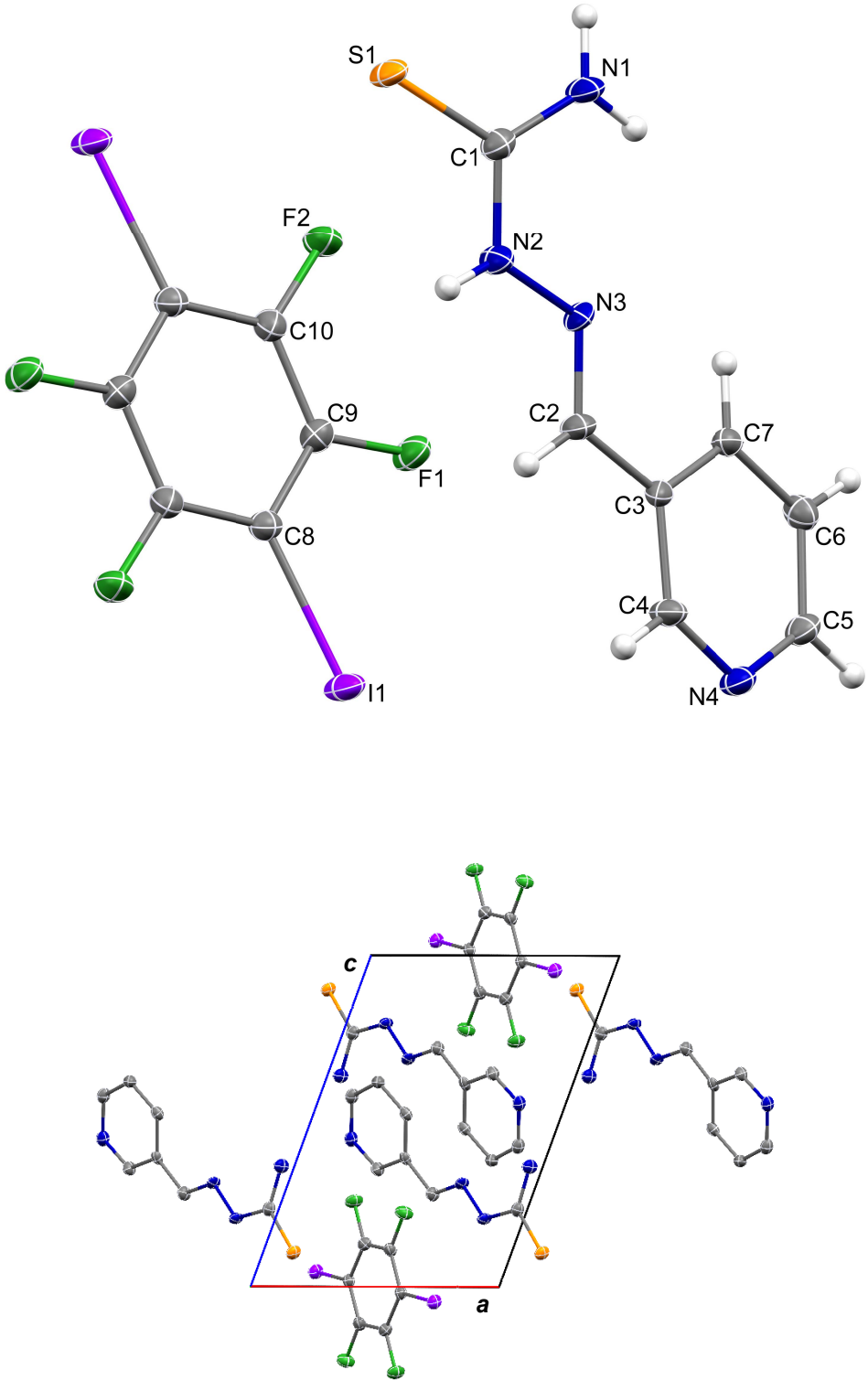

Figure SI11. Asymmetric unit (top) and unit cell packing (bottom) of **6C**. Hydrogen atoms are omitted for clarity. Atomic displacement ellipsoids are shown at the 50% probability level.

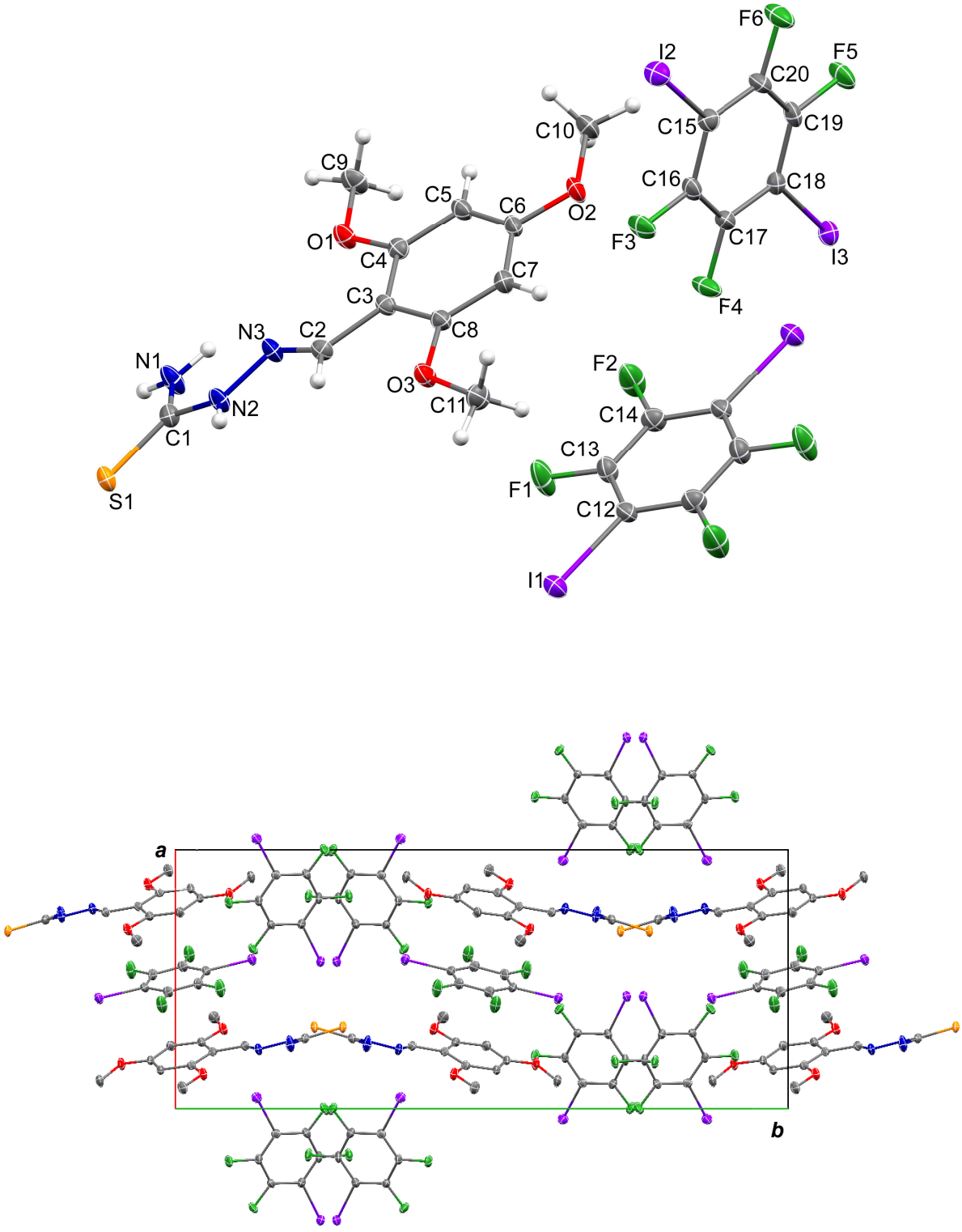

Figure SI12. Asymmetric unit (top) and unit cell packing (bottom) of **7C**. Hydrogen atoms are omitted for clarity. Atomic displacement ellipsoids are shown at the 50% probability level.

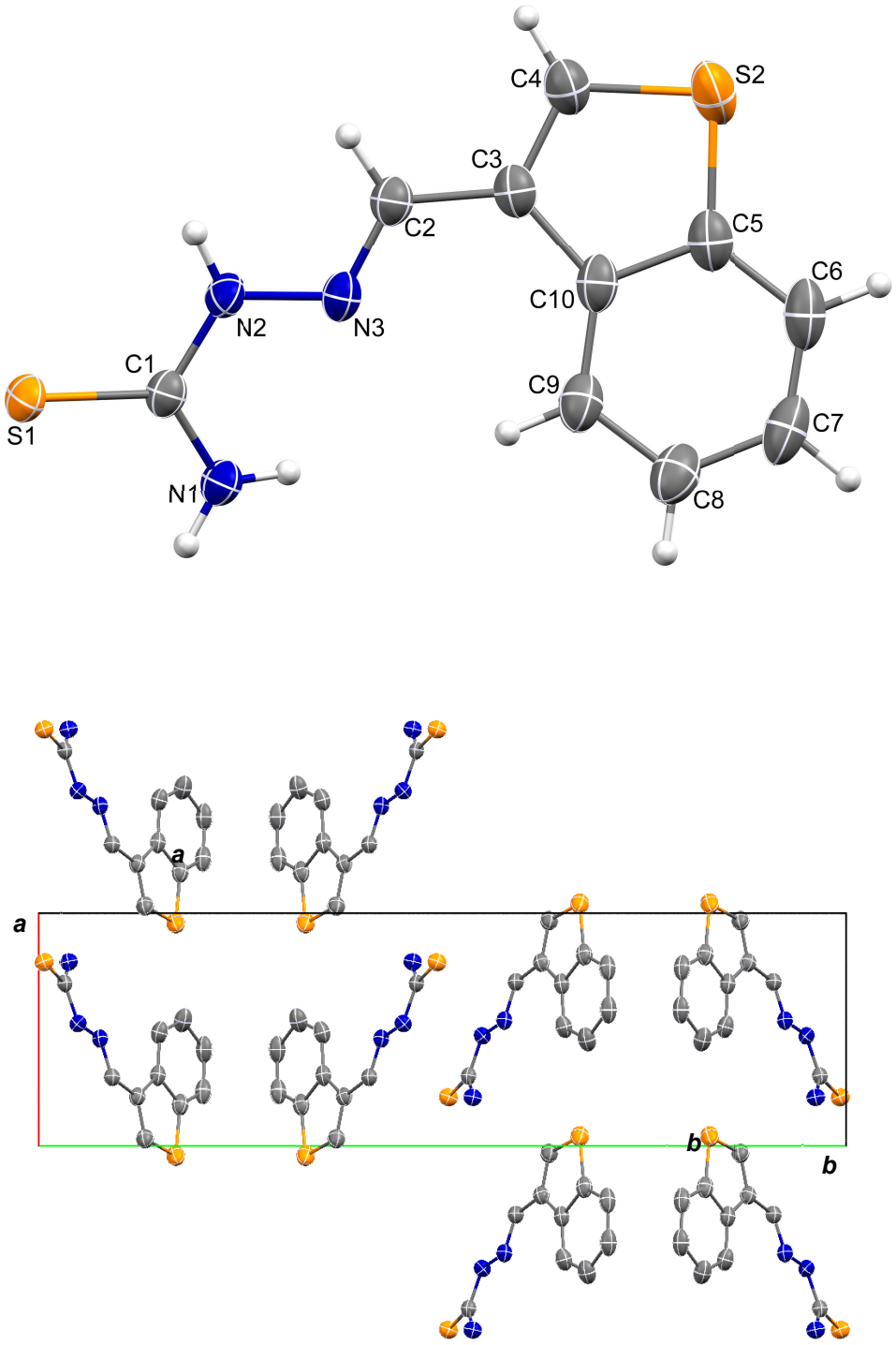

Figure SI14. Asymmetric unit (top) and unit cell packing (bottom) of **8**. Hydrogen atoms are omitted for clarity. Atomic displacement ellipsoids are shown at the 50% probability level.

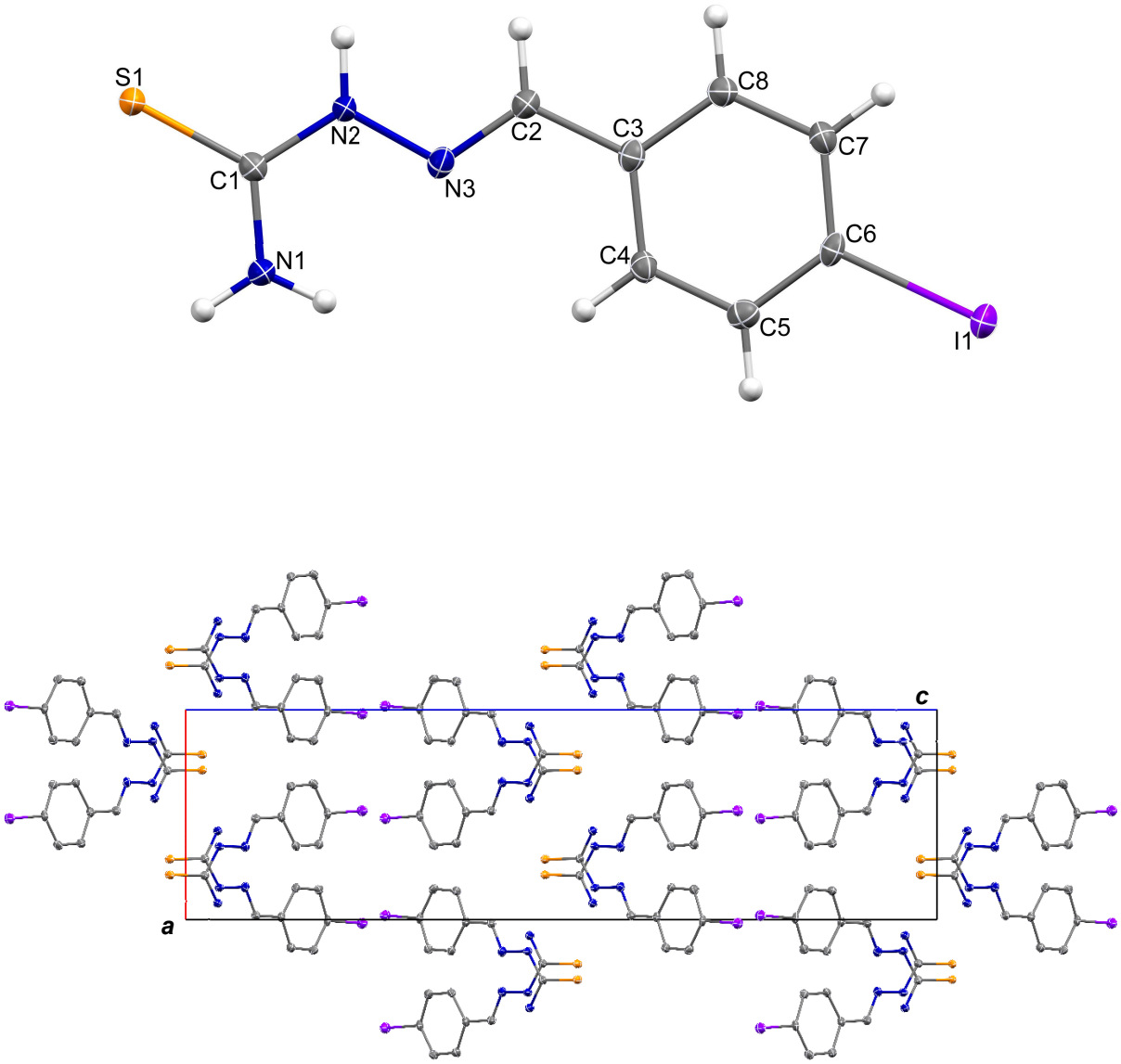

Figure SI15. Asymmetric unit (top) and unit cell packing (bottom) of **9**. Hydrogen atoms are omitted for clarity. Atomic displacement ellipsoids are shown at the 50% probability level.

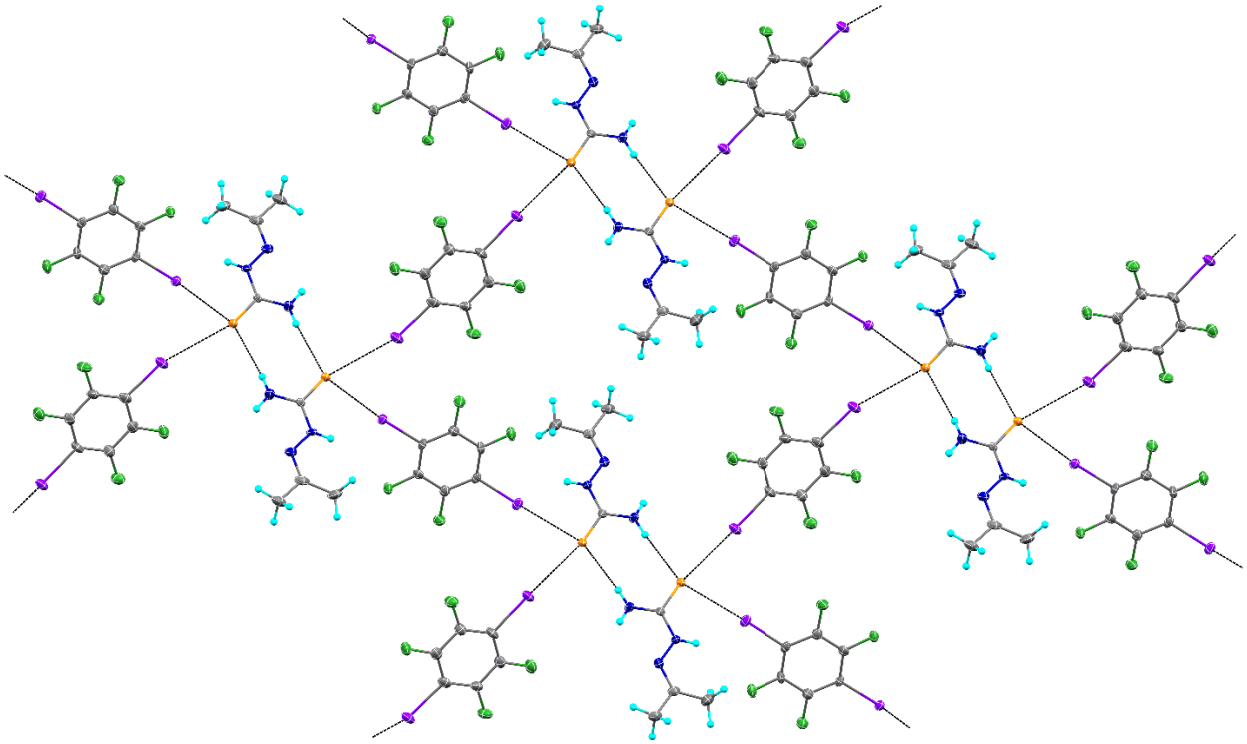

Figure SI16. Halogen and hydrogen bonding network in **1C**. Atomic displacement ellipsoids are shown at the 50% probability level.

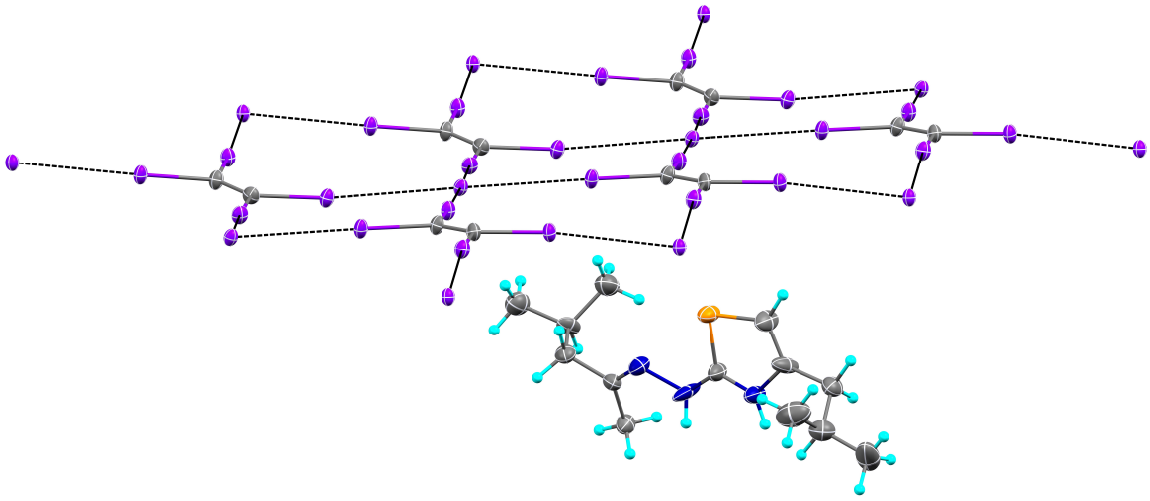

Figure SI17. Halogen bonding sheets in **2E**. Atomic displacement ellipsoids are shown at the 50% probability level.

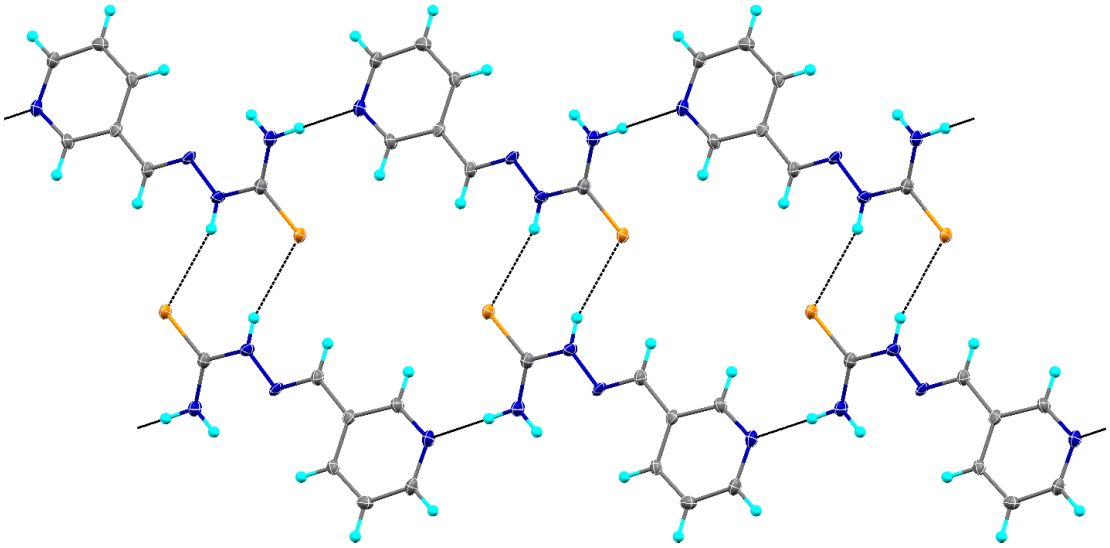

Figure SI18. Halogen and hydrogen bonding network in **6C**. Atomic displacement ellipsoids are shown at the 50% probability level.

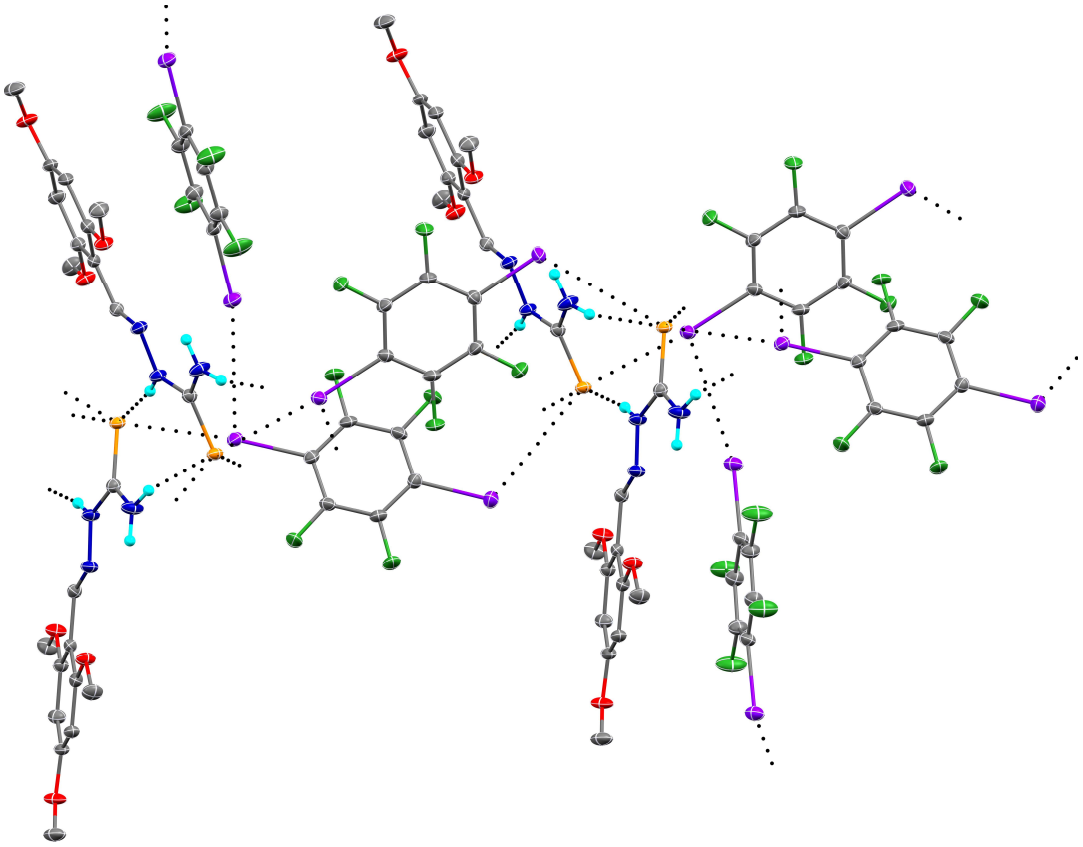

Figure SI19. Halogen and hydrogen bonding network in **6C**. Atomic displacement ellipsoids are shown at the 50% probability level.